Substrate Activation in the Urate Oxidase Reaction

A Thesis presented to the Faculty of the Graduate School

University of Missouri-Columbia

In Partial Fulfillment

Of the Requirements for the Degree

Master of Science

By

Charles G. Doll

Dr. Peter Tipton, Dissertation Supervisor

May 2008

Acknowledgments

Throughout the course of my thesis work at the University of Missouri, there have been many people that have influenced me. Professor Peter Tipton, my thesis advisor, has given me the opportunity to develop into a successful scientist. His ideas were the foundation for this project and his guidance was indispensable. Professors Linda Randall from the Biochemistry Department and Kent Gates from the Chemistry Department have served on my advisory committee. Their background has helped me explore my project from different angles. Dr. Randall's moral support helped me persevere. There are many others from the Biochemistry, Chemistry, and Geology Departments that have contributed to this project, who shared their knowledge, resources, and support. Professor Lesa Beamer and Professor David Emerich were apart of my original committee. Professor Cheryl Kelly and Damon Bassett from the Geology Department provided mass spectrometry facilities, expertise, and analysis of samples. Members of the laboratory, Dr. Agoston Jerga, Dr. Jennifer Kimmel, Laura Naught, Dr. Nick Power, and Dr. Aniruddha Raychaudhuri were an invaluable resource, who shared a diversity of knowledge and support. Although their names are not mentioned here there were many others that played an important role in my graduate career.

Table of Contents

LIST OF ILLUSTRATIONS

LIST OF TABLES

Tables **Page**

LIST OF SCHEMES

Schemes **Page**

Chapter 1. Introduction

1.1 Urate Oxidase

Urate oxidase (UO) is a unique enzyme that catalyzes the O_2-dependant oxidation of urate to 5-hydroxyisourate (Scheme 1-1) without the assistance of a metal ion or organic cofactor. UO is conserved in many organisms throughout nature. These organisms employ urate oxidase in many different processes. For example, UO is incorporated in an essential step of the nitrogen assimilation pathway in tropical legumes (Smith & Atkins, 2002). Most animals employ UO for the eradication of nitrogen waste by removing potentially toxic uric acid (Kakino *et. al*., 1998). Microorganisms such as *Bacillus fastidiosus* have been found to use urate as a main nitrogen and carbon source by the utilization of UO (Kaltwasser, 1971). Interestingly, in humans the gene encoding UO is interrupted by a single nonsense mutation producing an inactive gene product (Oda *et. al*., 2002). Because of this inactivation, build up of urate in chemotherapy patients can cause hyperuricemia, which can be treated with pharmaceutical UO (Patte *et. al*., 2002). The essential role that UO plays in nitrogen metabolism and the fact that few enzymes are known to catalyze O_2-dependant oxidation without a cofactor make urate oxidase an excellent choice for mechanistic studies.

Batelli and Stern were the first to isolate UO in 1909 (Holmberg, 1939). They showed that in the reaction of urate with UO one molecule of water and one molecule of oxygen are taken up and a molecule of allantoin and one molecule of carbon dioxide is formed. Other studies found that a molecule of H_2O_2 was formed during each round of catalysis (Keillin & Hartree, 1936). Mechanistic studies of UO continued through 1930's (Schuler

& Reindel, 1933), but low stability and purification yields made it difficult to determine. Early studies of UO created misconceptions about the reaction mechanism. In these early studies there were reports that iron or copper were essential for catalytic activity (Davidson, 1942; Mahler *et. al*., 1955). However, more recently it has been shown that urate oxidase does not require copper and that the addition of copper does not affect the rate of reaction (Kahn & Tipton, 1997). A second misconception frequently reported in the literature is that allantoin is the product of the urate oxidase reaction. Kahn has shown

Scheme 1-1.

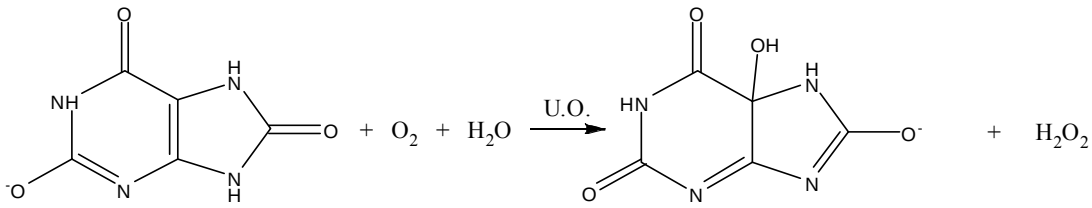

that the true product is 5-hydroxyisourate, which non-enzymatically degrades to allantoin with a half-life of 30 minutes (Kahn *et. al*., 1997). This short half-life had led to the previously false impression that allantoin was the product of the urate oxidase reaction. Additional studies have given evidence for other enzymes involved in the enzymatic catalysis of 5-hydroxyisourate to allantoin (Kahn *et. al*., 1997).

The fact that urate oxidase does not require a cofactor for activity (Kahn & Tipton, 1997) places it among a short list of cofactor independent oxidases including coproporophyrinogen III oxidase (Colloc'h *et. al*., 2002), tetracenomycin F1

monooxygenase (Shen & Huchinson, 1993), and ribulose 1,5-bisphosphate carboxylase (Cleland *et. al*., 1998). The lack of metal or organic cofactor has led to a proposed flavin-like mechanism (Kahn & Tipton, 1998) (Scheme 1-2).

Activation of many oxidases requires a flavin molecule to overcome the high redox potential of the spin-forbidden reaction of O_2 to H_2O_2 (Massey, 1994). Similarities between flavin and urate molecular structure allows us to draw analogies concerning the chemistry that occurs. In flavin oxidases a singlet reduced flavin and O_2 form a caged radical pair, which collapse to form a flavin hydroperoxide. Urate can be envisioned to form a dianion that could react with oxygen. We have proposed a mechanism in which urate is utilized in a manner similar to flavin oxidases forming the urate hydroperoxide intermediate (Scheme 1-2). Hydrogen peroxide is released from the intermediate and dehydrourate is produced. In the final step the dehydrourate is attacked by water to produce 5-hydroxyisourate.

Scheme 1-2.

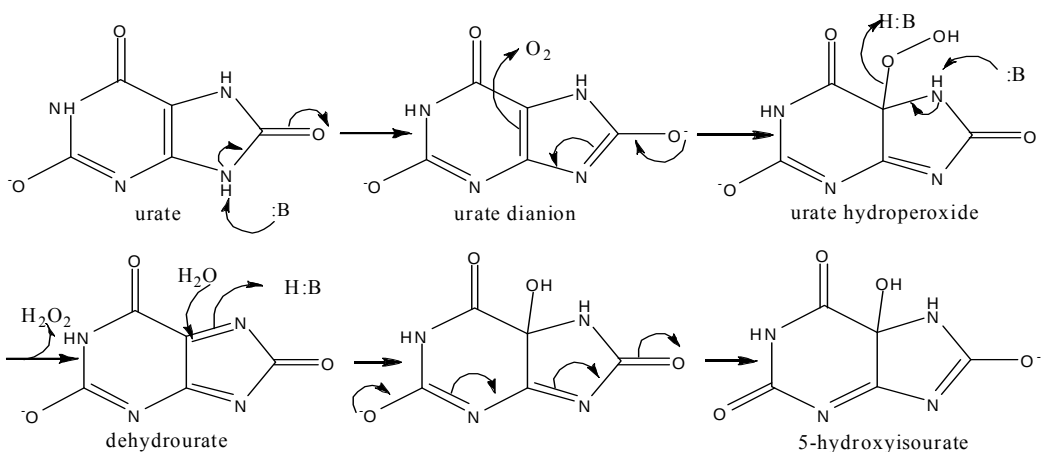

Evidence for two intermediates has been demonstrated by stopped-flow experiments (Kahn & Tipton, 1998). These methods monitored the products of the single turnover urate oxidase reaction. The absorbance of the first enzyme-bound intermediate, proposed to be urate dianion, was observed at 295 nm. The single turnover reaction products have a maximum absorbance at 298 nm, which is near that of the expected absorbance for urate hydroperoxide.

Further evidence that a urate hydroperoxide intermediate occurs in a reaction between the urate dianion and O_2 is provided by intermediate trapping experiments (Sarma & Tipton, 2000). Isotope labeled $H_2{}^{18}O$ experiments in the presence of DTT did not show oxygen labeling at the C4 position, confirming that oxidation must be derived from oxygen and not solvent.

The crystal structure of *Aspergillus flavus* urate oxidase has been previously determined (Colloc'h *et. al*., 1997) to be a tetramer with 8-azaxanthine bound in the active site (Figure 1-1). Figure 1-2 is an illustration of the structure of the active site. Although no structures of the *Bacillus subtilis* UO are available, conservation of active site residues between species allow us to assign the roles of the *B. subtilis* amino acids. This structure has been used to choose amino acid residues thought to be involved in the binding and catalysis of the urate oxidase reaction for site directed mutations. A number of site directed mutational studies have been conducted on *B. subtilis* urate oxidase to determine the involvement of active site residues. Of particular interest are the active site mutations T69A, K9M, F179A, Q245A, and R196A, all of which had a large reduction in activity compared to the wild type enzyme (Imhoff *et. al*., 2003). These active site residues are thought to play a direct role in the binding of urate and catalysis.

Figure 1-1: Crystal structure of urate oxidase tetramer.

Top View

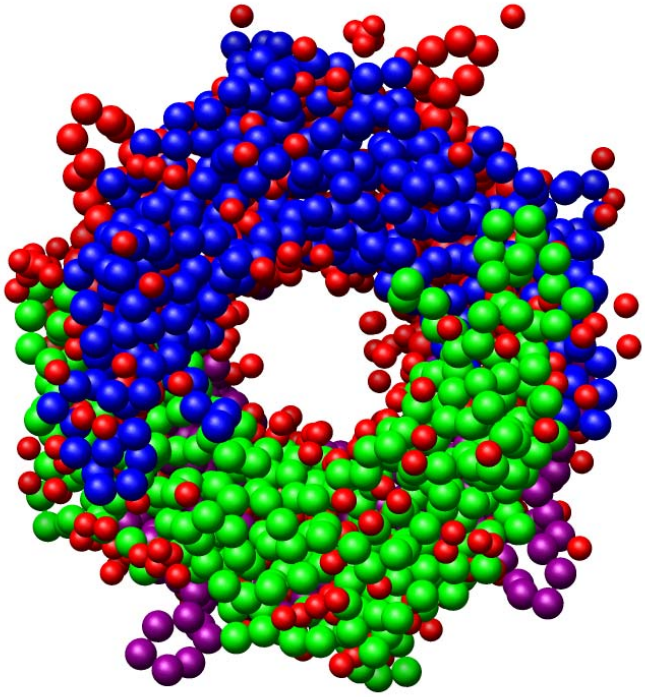

Side View

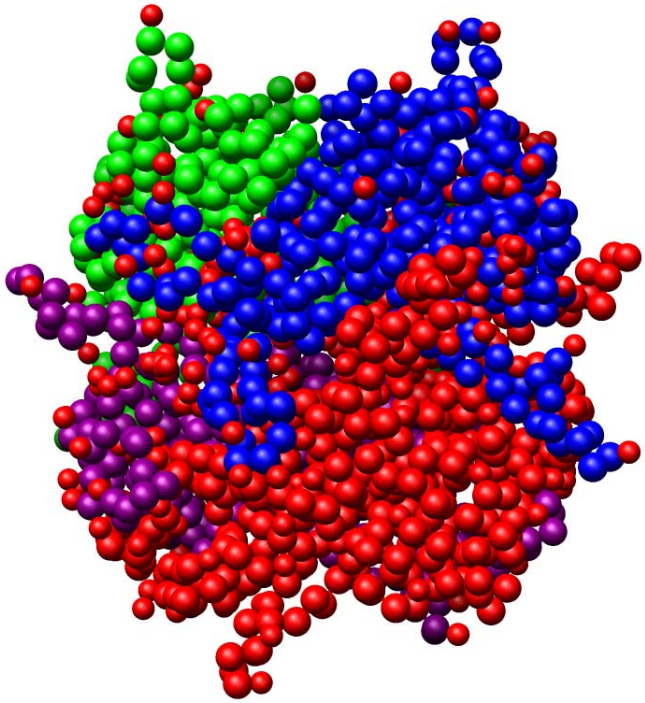

Figure 1-2: Crystal structure of urate oxidase active site with the inhibitor 8-azaxanthine bound.

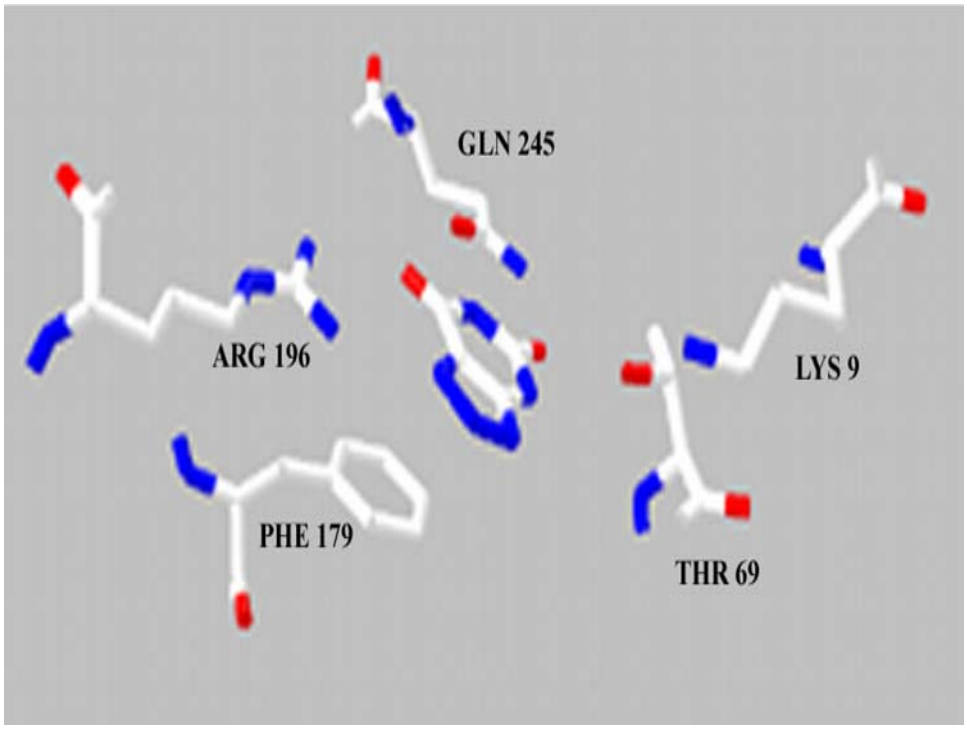

To form the proposed urate dianion, a proton is thought to be extracted from the N9 position of urate. T69 and K9 are believed to act as a catalytic diad to extract the N9 proton and form the urate dianion (Imhoff *et. al*., 2003). F179 may be involved in pi-stacking interactions with the substrate. This stacking may lower the midpoint potential, as in flavin chemistry (Breinlinger & Rotello, 1997), and help facilitate the transfer of an electron from oxygen to urate. The residues Q239 and R196 could be involved in substrate recognition but the reductions in V_{max} of the Q239A and R196A mutants to 0.44% and 0.12% respectively indicates that they also have a function in catalysis.

Further binding studies utilizing U.V. visible spectroscopy of the competitive inhibitor 8-nitroxanthine provides evidence of interactions between the substrate and the UO active site. A shift in the maximum absorbance of 8-nitroxanthine from 379 nm when free in solution to 399 nm bound to enzyme has been measured (Figure 1-3). This shift in absorbance is indicative of changes in the chemical reactivity of the enzyme-bound substrate resulting from changes in vibrational and electronic properties.

The vibrational changes of the bound and unbound 8-nitroxanthine to UO were further examined with Raman spectroscopy (Doll *et. al*., 2005). These studies were performed in Dr. Peter Tonge's laboratory at SUNY Stonybrook. A vibrational shift between the bound and unbound 8-nitrozanthine was observed in the peak corresponding to the C4-C5 stretching mode from 1545 cm^{-1} to 1541 cm^{-1} (Figure 1-4). This shift is indicative of increasing bond length between C4 and C5 of 8-nitroxanthine resulting in a C4-C5 bond having more single bond character. Another interesting finding was that the bound 8-nitroxanthine is transformed to the dianionic form. This can be detected by the

appearance of Raman peaks at 577 and 530 nm (Figure 1-5). In the inactive F179A and K9M mutants the dianion is not formed.

A higher resolution crystal structure of *Aspergillus flavus* UO has been determined with several inhibitors bound (Retailleau *et. al*., 2005). Crystal structures of UO with uracil, 5,6-diaminouracil, 5-amino-6 nitrouracil, and guanine bound all had similar backbone structures the most significant differences in the active site orientation (Figure 1-6). Guanine is the most similar in structure to the natural substrate. When guanine is bound to UO it is bound in the active site flipped with respect to the orientation of 8-azazanthine in the previously solved structure (Retailleau *et. al*., 2005; Colloc'h et. al., 1997). This variance in orientation presents the question of the orientation of urate when bound. Interestingly, it seems that the more similar the inhibitor is to the substrate the more it stabilizes the interface at the active site between the each dimmer allowing for a better diffraction. This may indicate that the better the transition state analog the more tightly the inhibitor binds.

Figure 1-3. U.V. spectra of the inhibitor 8-nitroxanthine bound to UO and free in solution.

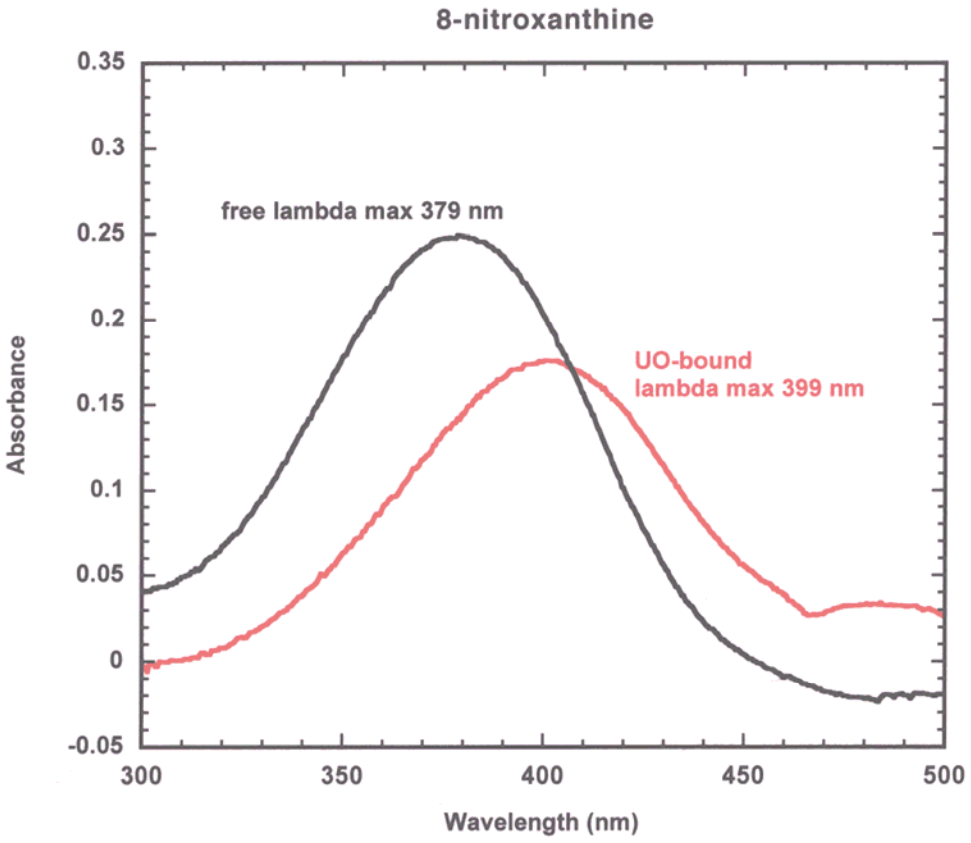

Figure 1-4. Raman spectra of the inhibitor 8-nitroxanthine bound to UO and free in solution.

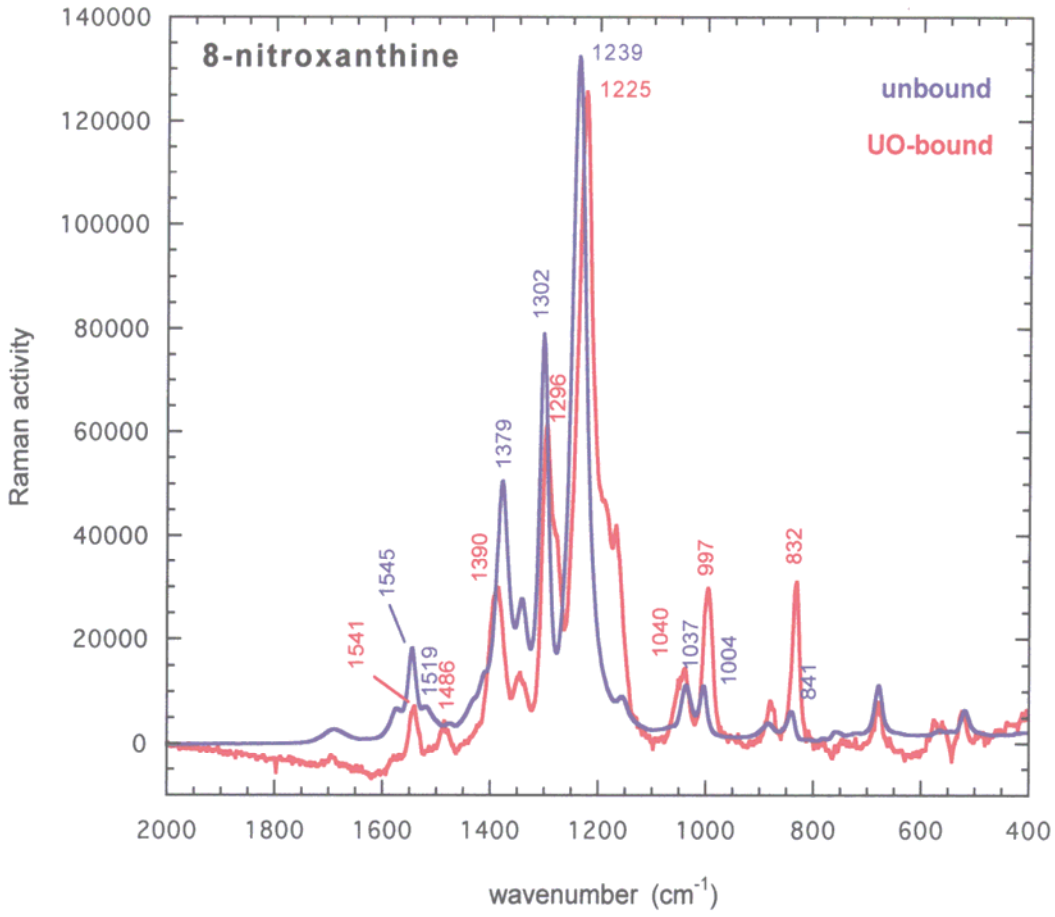

Figure 1-5: Comparison of Raman difference spectra for the F179Y, F179A, and K9M mutants (solid line) with wild type U.O. (dotted line) in the 450-650 cm^{-1} region (upper) and the 1545-1541cm^{-1} region (lower).

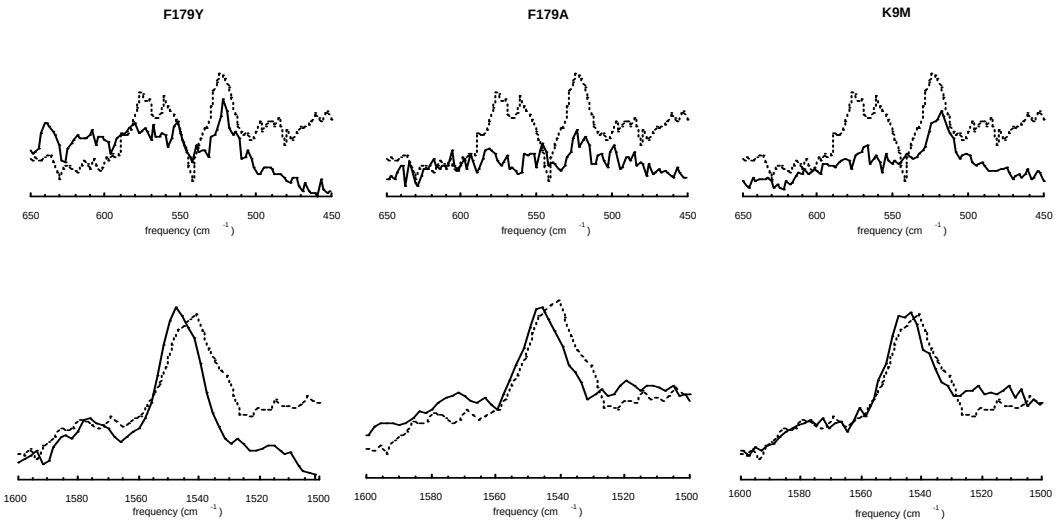

Figure 1-6: The inhibitor is flipped in the active site of the most recent structure compared to the previous structure.

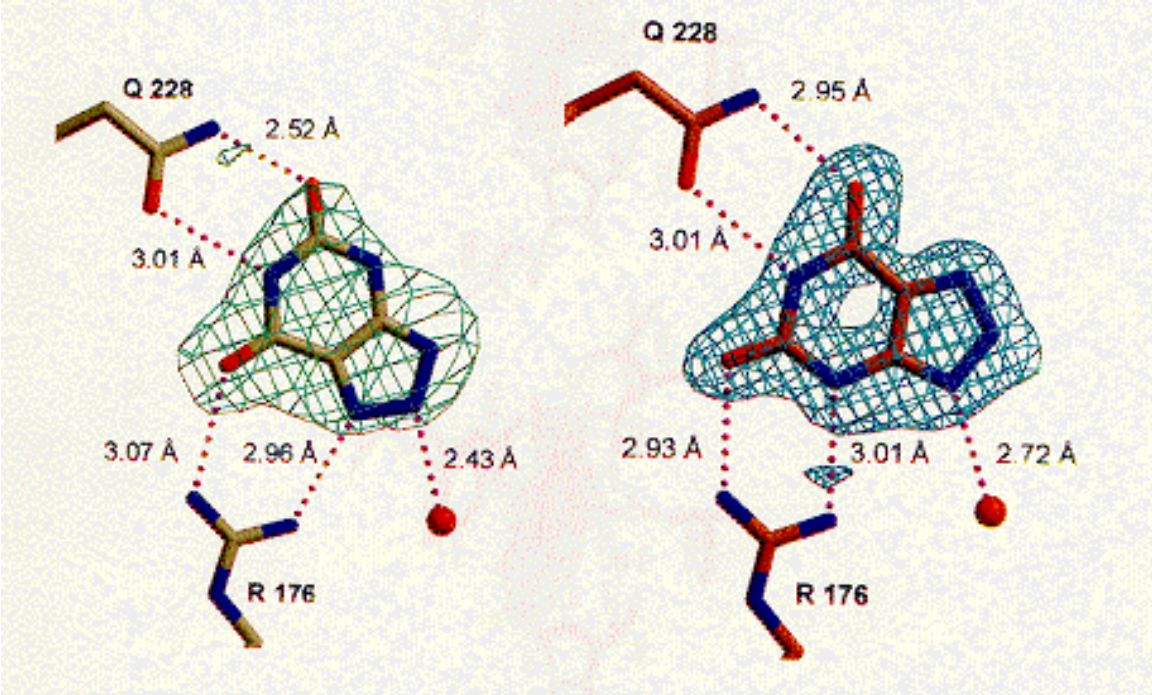

Previous **New**

1.2 Kinetic Isotope Effects

Lowering of the transition state energy of a reaction is one of the key strategies that an enzyme incorporates in order to increase the rate of catalysis. Therefore, determination of the transition state structure can give insight into the manner of which an enzyme achieves catalysis. Currently kinetic isotope effects (KIE) are the only method available to directly probe the transition state structure. An isotope effect (IE) is a change in the ratio of rates or equilibrium constants upon the substitution of a heavy isotope in place of the naturally occurring light isotope in the substrate. An example of this substitution would be, ^{13}C exchanged for ^{12}C. This substitution changes the bond vibrational frequency. KIE's are differences in the ratio of rates of a reaction between substrates with different isomers at an isotopically sensitive position ($^{12}k/^{13}k$, where ^{12}k and ^{13}k are rates for the reaction with ^{12}C and ^{13}C respectively). A KIE will only occur at positions in which a bond is made, broken, or the bond character changes in the transition state. The harmonic oscillator is a good model for demonstrating the relationship between the mass of an atom and its bond vibrational frequency:

$$\omega_0 = \sqrt{\frac{C}{m}} \qquad (1\text{-}1)$$

where C is the spring constant, m is mass, and ω_o is the vibrational frequency. A change in mass from the substitution of a heavy isotope will result in lowering the vibrational energy of the molecule. This lower energy results in a lower initial resting energy for the molecule (Figure 1-7). When this change in energy is at a position that is involved in the reaction it results in a change in the energy that the molecule must overcome to form

products (Figure 1-7). These changes are very small, therefore the direct comparison method in which the kinetic parameters of reactions with labeled and unlabeled substrate are compared is not sensitive enough to detect them. The competitive method is a more sensitive method for the measurement of measuring isotope effects (O'Leary, 1980). This method measures changes in the ratio heavy and light isotopes at an isotopically sensitive position as the reaction proceeds. These differences can be determined by measuring the change of $^{13}C/^{12}C$ in the substrate and in the product after a partial reaction of 20-40% completion (Cleland, 1987). By measuring the KIE of urate on the UO reaction, insight into the transition state structure of the reaction can be obtained.

To determine the observed KIE from the competitive method, the relationship below is used:

$$^{13}(V/K) = \frac{\log(1-f)}{\log(1-f\,R_P/R_0)} \qquad (1\text{-}2)$$

Where ^{13}(V/K) is the ^{13}C KIE on V/K, f is the reactions fraction of completion, R_p is the ratio of $^{12}C/^{13}C$ in the product, and R_0 is the ratio of $^{12}C/^{13}C$ in the initial substrate. If there was no KIE for the reaction, the ^{13}(V/K) value would be unity. If $^{12}k > {}^{13}k$ a "normal" isotope effect where ^{13}(V/K) > 1.0 is observed. Inverse KIE, where ^{13}(V/K) < 1.0, may occur due to an inverse equilibrium IE on binding. The observed KIE can also be related to commitment factors and the intrinsic isotope effect:

$$^{13}(V/K) = \frac{(^{13}k + c_f + c_r\,{}^{13}K_{eq})}{(1 + c_f + c_r)} \qquad (1\text{-}3)$$

Where ^{13}k is the intrinsic isotope effect for the reaction, $^{13}K_{eq}$ is the equilibrium isotope effect on the overall reaction, c_f is the forward commitment factor, and c_r is the reverse commitment factor. Commitment factors are defined as the ratio of the rate constant for the isotope sensitive step to the net rate constant for the release of reactant from the enzyme (Cleland, 1987). Equation 1-5 and 1-6 are the forward and reverse commitment factors for the mechanism below in which k_5 and k_6 are the isotope sensitive step.

$$E \underset{k_2}{\overset{k_1 A}{\rightleftharpoons}} EA \underset{k_4}{\overset{k_3}{\rightleftharpoons}} EA^* \underset{k_6}{\overset{k_5}{\rightleftharpoons}} EPQ^* \underset{k_8}{\overset{k_7}{\rightleftharpoons}} EPQ \xrightarrow{k_9} EQ \xrightarrow{k_{11}} E \qquad (1\text{-}4)$$

$$c_f = (k_5 / k_4)(1 + k_3 / k_2) \qquad (1\text{-}5)$$

$$c_r = (k_6 / k_7)(1 + k_8 / k_9) \qquad (1\text{-}6)$$

Commitment factors and equilibrium isotope effects in enzyme reactions usually mask the intrinsic isotope effect. One method to determine the intrinsic isotope effect for muti-substrate reactions is to measure the KIE for a reaction with different concentrations of the substrate not being analyzed. A plot is made of the observed KIE vs. substrate concentration and the line is extrapolated to zero concentration. When the substrate concentration is zero, the commitment factors would be reduced to zero. Since commitment factors are related to rate constants, the observed KIE would be equal to the intrinsic KIE (Cleland, 2006). To determine the transition state structure the intrinsic isotope effect can be compared to proposed transition state structure calculations from molecular modeling programs, such as Gausian. These comparisons will determine the validity of the proposed transition state structure.

Figure 1-7: The resting energy is lower for a substrate with a heavy (H) isotope compared to one with a light (L) isotope. This difference increases the energy required for substrate to form a product.

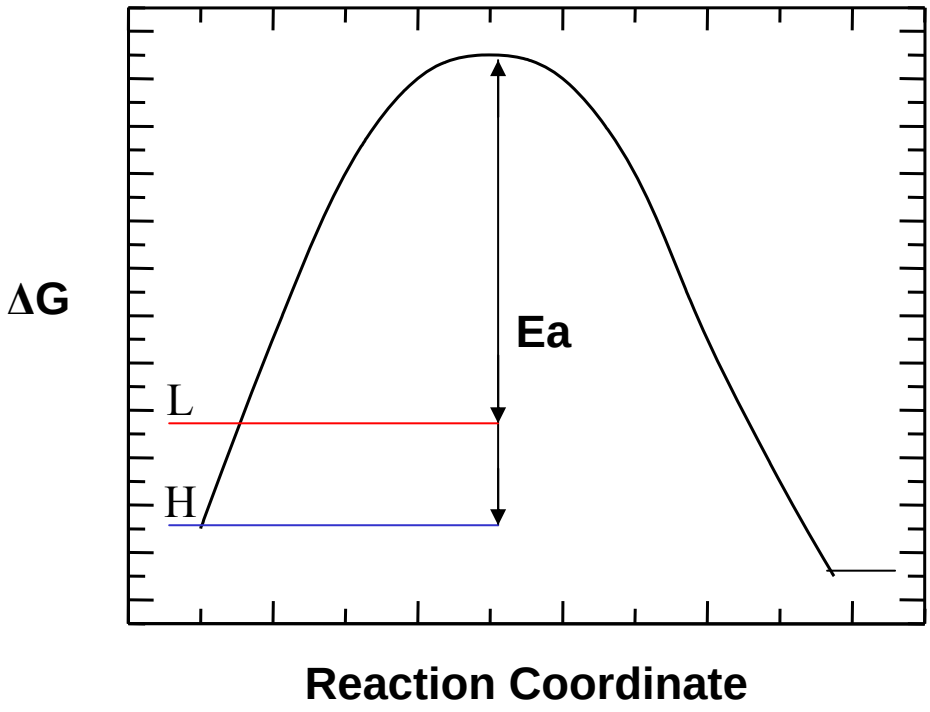

D-amino acid oxidase has been studied using KIE techniques (Kurtz *et. al*., 2000). D-amino acid oxidase is a flavoprotein that catalyzes the oxidation of α-amino acids and ultimately results in the elimination of HCl from β-chlorinated amino acids. The reaction catalyzed by D-amino acid oxidase has been investigated using ^{15}N KIE of the serine substrate to distinguish between two possible reaction mechanisms (Kurtz *et. al*., 2000). Kurtz investigated the first step in the elimination of HCl, the extraction of the α-hydrogen of the amino acid and formation of the imino acid. The first proposed mechanism involved the formation of the imino acid through a carbanion intermediate (Scheme 1-3). Another possibility was that the imino acid is formed by a direct hydride transfer from the amino acid to the flavin (Scheme 1-4). The secondary ^{15}N KIE of 0.9963±0.0016 was measured for the serine reaction with D-amino acid oxidase. This measured value correlated with a calculated inverse KIE value of 0.997 as opposed to the expected value of 1.000 or larger for the carbanion mechanism. Therefore, the measured KIE supported a direct hydride transfer in imino acid formation (Scheme 1-4).

Scheme 1-3

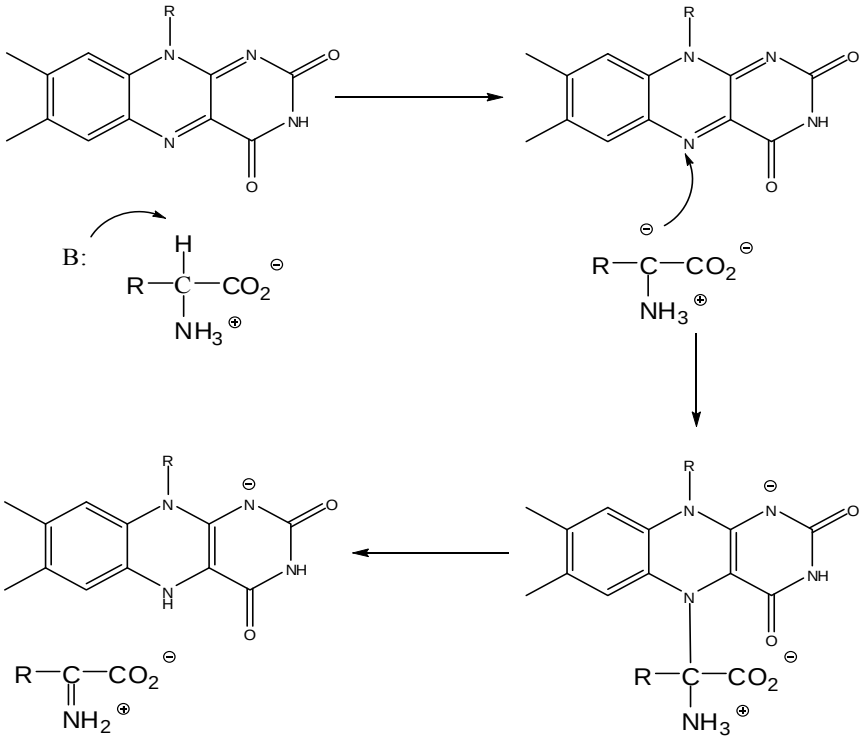

Scheme 1-4

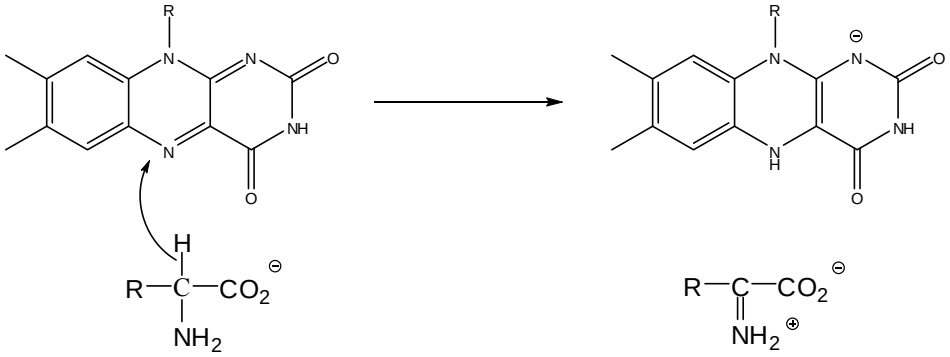

1.3 Solvent Isotope Effects

Solvent isotope effects (SIE) are an additional isotope effect technique that takes advantage of kinetic differences that occur due to isotopic alteration. SIE's are rate or equilibrium differences resulting from solvent exchange. For example, H_2O and D_2O are isotopic alterations of one another. SIE's have been employed to give evidence for proposed chemical events that occur in the reaction mechanism (Theodorou et. al., 2001; Gandour, 1980). The origin of SIE's is the exchange of proton to deuterium atoms at solvent exchangeable sites throughout the enzyme. Proton exchange often results in measurable SIE's with IE values that are often >2 in magnitude (Schowen, 1979).

The proton inventory (PI) method has been used to determine the number of protons in flight during one round of catalysis before the rate determining step (Schowen, 1982). A PI is created by measuring the kinetic parameters for a reaction in solvents of varying isotopic compositions. A graph is obtained by plotting k_n/k_0 or $(V/K)_n/(V/K)_0$, where k_0 is the rate in H_2O and k_n is the rate in solvent of composition n, vs. the mole fraction of D_2O. The deviation from linearity in the PI plot is coupled to the number of protons in flight. A linear PI corresponds to one proton in flight. Curvature of the PI indicates that the SIE is due to more than one proton. The Gross-Butler equation is commonly used to fit PI data for a mathematical interpretation of the number of protons involved:

$$ {}^{n}k = {}^{0}k \frac{\prod_{i}^{x}(1-n+n\phi_i^T)}{\prod_{i}^{x}(1-n+n\phi_i^R)} \qquad (1\text{-}7) $$

where ${}^{n}k$ is the rate measured in isotopic mixtures (n) of H_2O and D_2O, ${}^{0}k$ is the rate in H_2O, ϕ_i^T and ϕ_i^R are isotopic fractionation factors for the transition state (T) and the reaction state (R) respectively. All the transition-state hydrogenic sites, *i*, that contribute to the SIE in the reaction are accounted for in the numerator. The denominator similarly contains all the exchangeable reaction state protons. In the reactant state all sites are exchangeable with solvent, therefore it is commonly assumed that $\phi_i^R=1$ and the denominator becomes unity. With this assumption equation 2 is simplified to:

$$ {}^{n}k={}^{0}k\prod_{i}^{x}(1-n+n\phi_i^T) \qquad (1\text{-}8)$$

A single proton exchange would result in Equation 1-9,

$$ {}^{n}k={}^{0}k(1-n+n\phi) \qquad (1\text{-}9)$$

resulting in a linear PI plot. A SIE arising from two protons in flight would result in two possible scenarios each producing quadratic equations. In the first situation $\phi_1 = \phi_2$ and:

$$ {}^{n}k={}^{0}k(1-n+n\phi)^2 \qquad (1\text{-}10)$$

The second variation $\phi_1 \neq \phi_2$ results in Equation 1-11.

$$ {}^{n}k={}^{0}k(1-n+n\phi_1)(1-n+n\phi_2) \qquad (1\text{-}11)$$

This can be continued to create mathematical equations for systems of more than two protons involved in the net SIE. Because the difference between a fit of 3 or greater becomes very small, it is difficult to distinguish between 3 or more protons in flight using the PI method.

The proposed catalytic diad in the UO reaction mechanism makes PI an ideal method to study the number of protons in flight. One proton is proposed to be extracted from threonine by lysine while at the same time threonine is abstracting a proton from the

substrate, therefore the catalytic diad would be expected be responsible for two protons in flight.

Asparaginase and glutaminase catalyze the hydrolysis of asparagine and glutamine (Scheme 1-5). These enzymes are proposed to use a catalytic triad in hydrolysis (Quinn *et. al*, 1980; Ortlund *et. al*, 2000). PI was used to study the number of protons in flight for reactions of asparaginase and glutaminase with natural and unnatural substrates (Quinn *et. al*, 1980). In these studies curvature in PI indicated that more than one proton was in flight during a round of catalysis. The Gross-Butler equation (Equation 1-7) was used to further analyze and compare the PI of reactions with natural and unnatural substrates. Quinn used a technique developed by Albery which compares the midpoint partial SIE, where n=0.5, with calculated predictions for one and two protons in flight, along with a general solvation model. They found that for natural substrates, the measured midpoint SIE was between the predicted values for two protons and general solvation. If the square root of Equation 1-10 is rearranged, a straight line equation results. A plot of the square root of the SIE vs. n was linear, indicating that the data was consistent with a two proton transfer. Asparaginase was also studied with glutamine and succinamate as the substrate. The reaction with glutamine was found to have only one proton in flight while the reaction with succinamate was consistent with two protons in flight. It is possible that glutamine (Figure 1-8), which is longer than asparagine, does not fit into the active site of asparaginase therefore limiting the enzymes interaction with the substrate and reducing the number of observed protons in flight. Conversely, succinamate, which has one less amino group than asparagine (Figure 1-8), would be expected to easily fit into the active-site. This PI study gave evidence for multiple protons

in flight that were predicted for a catalytic diad. It also indicated that a proper fit between substrate and the active site was necessary for the full catalytic power.

Scheme 1-5

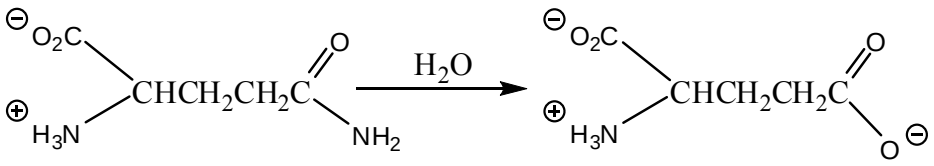

Asparaginase

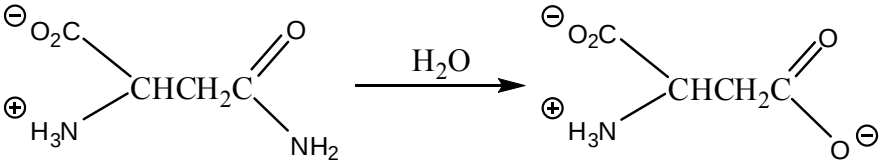

Glutaminase

Figure 1-8: Structure of asparagine (1), succinamate (2), and glutamine (3).

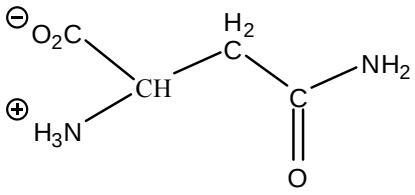

1

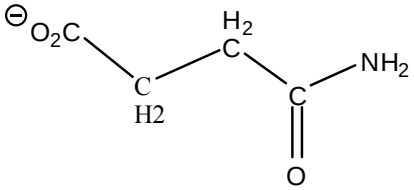

2

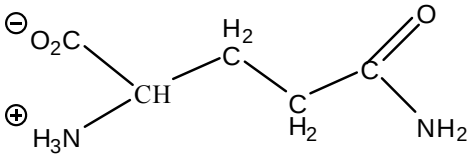

3

1.3 Research Objective

The main goals of this research project were:

1. Develop new methods for measuring KIE's with continuous flow mass spectroscopy and ^{13}C-depleted substrates.
2. Use the proton inventory method to look at the number of protons in flight.

Chapter 2. Carbon Kinetic Isotope Effects

2.1 Introduction

Isotope effects are currently the only method of determining the transition state structure of a reaction mechanism. A common way of measuring isotope effects in enzymatic systems is the competitive method. This method measures the change in the isotopic ratio of one atom in the substrate and the product of a reaction that has been run to partial completion (O'Leary, 1980). To measure the isotope effect at a specific atom center, the atom of interest must be individually isolated. We have developed a method of degrading the product of the urate oxidase reaction, 5-hydroxyisourate, to glyoxylate, which contains two carbons originating from the C4 and C5 positions of urate (Scheme 2-1). By synthesizing urate with ^{13}C-depleted C4 or C5, the $^{13}C/^{12}C$ isotope ratio at either carbon can be measured using a continuous flow mass spectrometer (available through collaboration with Dr. Kelley in the Geology Department University of Missouri-Columbia).

Scheme 2-1

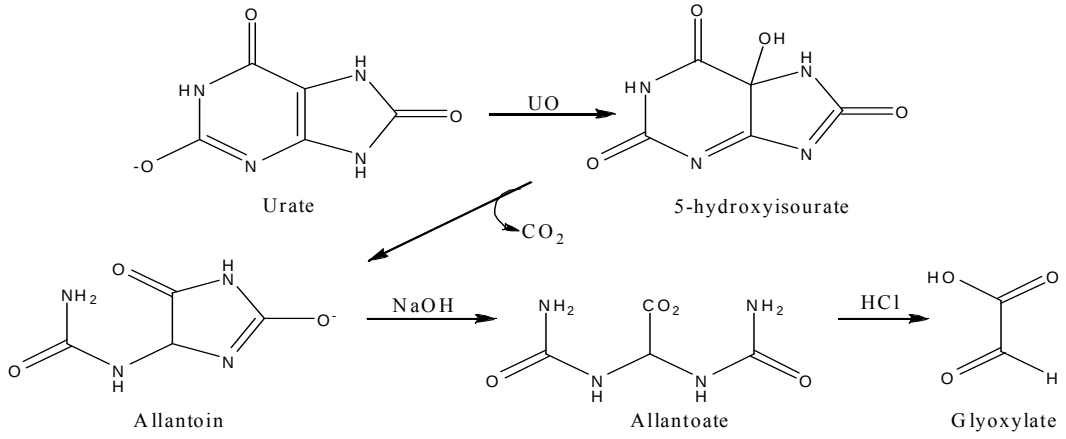

Urate can be synthesized with commercially available ^{13}C-depleted cyanide to produce urate that is ^{13}C-depleted at position C4 as shown in Scheme 2-2 (Kahn *et. al*., 1997). Similarly, urate that is ^{13}C-depleted at position C5 can be produced by first synthesizing bromoacetic acid from ^{13}C-depleted acetic acid and N-bromosuccinimide (Zhang *et. al*., 1998). This bromoacetic acid is then used in the synthesis of ^{12}C5 urate as above.

The research conducted to date creates a strong background supporting the proposed flavin-like mechanism for urate oxidase (Kahn *et. al*., 1997). Supportive research include evidence of the dianion and urate hydroperoxide intermediates (Khan *et. al*., 1998), the *Aspergillus flavus* crystal structure, mutational studies (Collech *et. al*., 1997), and Raman spectroscopy results (Doll *et. al*., 2005) support the proposed flavin-like mechanism. This foundation of knowledge has laid the groundwork for the use of isotope effect experiments to expand upon the understanding of this unique enzyme.

Naturally abundant ^{13}C kinetic isotope effects at positions 4 and 5 of urate were determined by comparing the ^{13}C/^{12}C ratio at each position in the substrate, urate, and the reaction product after being run to partial completion. The competitive method developed by O'Leary (O'Leary, 1980), in which the isotopic composition of the starting material and the product are compared, was used to measure kinetic isotope effects. To measure the isotopic composition in the product, urate oxidase reactions were allowed to proceed to 100% completion and the ^{13}C/^{12}C ratio in the product was measured. The ^{13}C/^{12}C ratio from a reaction allowed to progress to 20% completion was compared to that of the 100% completion reaction. The resulting 5-hydroxyisourate product stood at room temperature overnight to facilitate non-enzymatic decomposition to allantoin. Allantoin can be

degraded to glyoxylate (Scheme 2-1) (Vogels and van der Drift, 1970), which contains the C4 and C5 originating from urate. We have adapted these methods for our measurements. The $^{13}C/^{12}C$ ratio in glyoxylate can be measured with sufficient precision for isotope effect comparisons using continuous flow mass spectrometry (Matthews and Hayes, 1978). To distinguish the isotope effects occurring at the C4 and C5 position, urate was synthesized using ^{13}C-depleted cyanide. That way, the C4 position of urate was unlabeled and the observed isotope effect was due to ^{13}C originating from the C5 position of urate. The isotope effect resulting from the C4 position of urate can be calculated by two methods. One method would be by repeating the experiment with authentic urate and comparing the difference between the ^{13}C depleted and authentic urate isotope effect. The second method would be to synthesize urate with ^{13}C-depleted bromoacetic acid.

For modeling of the transition state structure, the value of the intrinsic isotope effect for the reaction is needed. To determine the intrinsic isotope effect, whole molecule $^{18}(V/K)$ KIE experiments were conducted. In these experiments, $^{18}(V/K)$ was determined with several different concentrations of the substrate oxygen. Because oxygen is one of the substrates of the reaction, changing the concentration will affect the commitment factors and equilibrium of the reaction. As the substrate concentration is decreased the commitment factors and equilibrium isotope effect will decrease proportionally. A plot of $^{18}(V/K)$ vs. oxygen concentration was constructed. From this plot the intrinsic KIE of the reaction as be determined by extrapolating to zero oxygen concentration where $^{13}(V/K)$ is equal to ^{13}k (Equation 1-3).

In this study, we began developing methods to determine the $^{13}(V/K)$ KIE at positions C4 and C5 of urate using continuous flow MS.

2.2 Methods

General Reagents

Urate, allantoin, glyoxoylic acid, PMSF, TLCK, protoamine sulfate, DNaseI, lysosyme, xylenol orange, hydantoase, lactate dehydrogenase, phenol, and nitroprusside were purchased from Sigma Chemical Company. Luria broth (LB) was purchased from Research Products Inc., IPTG and Tris buffer were purchased from Research Organics. Ammonium persulfate, NaH_2PO_4, ampicillin, $MgSO_4$, $CaCl_2$, HCl, NaOH, $NaIO_4$, and chloroform were purchased from Fisher Scientific. Protein assay solution and AG1-X8 resin (Dowex) were purchased from BioRad. ^{13}C-depleted cyanide and ^{13}C-depleted acetic acid were purchased from Cambridge Isotope Laboratories Inc. Bleach was purchased from Novel Wash. Oxygen for reactions was supplied by Praxair. BL21(DE3) cells were purchased from Invitrogen.

Purification of Urate Oxidase

Over expression. The gene encoding urate oxidase from *Bacillus subtilis* was previously cloned into pET-14b vector with a $(His)_6$-tag at the N-terminus (Imnoff ***et. al***., 2003). *Escherichia Coli* BL21-(DE3) competent cells were transformed by adding 2 ul of plasmid to 20 µl BL21-(DE3) cells and incubating for 20-30 minutes on ice. The cells were heated in a water bath at 42˚C for 50 seconds, and then 500 µl LB media was added. The cells were allowed to incubate at 37˚C for 1 hour. After incubating, 60 µl of the culture was plated onto a LB ampicillin plate and grown overnight at 37˚C. One colony

from the plate was transferred to 2 ml of LB growth media containing 100 µg/ml ampicillin. This growth was transferred to 50 ml and 450 ml cultures. Six liters of media were induced with approximately 450 µl of culture and grown to an $O.D._{600\text{-}800}$. Overexpression was induced by the addition of 95 mg/L IPTG. The cells were allowed to grow overnight at 25˚C. The cells were harvested by centrifugation at 10,000 rpm. Pelleted cells were stored at -80˚C until purification.

Purification. 30 grams of cell paste was resuspended in 120 ml 50 mM Tris buffer pH 8.0 containing 2 mM $MgSO_4$, 2 mM $CaCl_2$, 0.5 mM TLCK, 0.5 mM PMSF, 24 mg lysozyme, and 240 µg DNaseI. The cells were incubated at 37˚C in a water bath with shaking for 30 minutes and then sonicated for 10-20 seconds for cell disruption. Cell debris was removed by centrifugation at 17,500 g for 45 minutes. 90 mg of protamine sulfate was dissolved in 9 ml H_2O and this solution was added dropwise with stirring to the supernatant on ice. The solution was stirred for an additional 15 minutes. Nucleic acids were removed by centrifugation at 15,000 g for 15 minutes. The supernatant was placed on ice and ammonium sulfate was added to 30% saturation (16.4 mg/ml). The solution was stirred for an additional 15 minutes and then centrifuged at 15,000 g for 15 minutes. The pellet was discarded. Again, the supernatant was placed on ice and ammonium sulfate was added to 55% saturation (14.8 mg/ml). The solution was stirred for an additional 15 minutes and then centrifuged at 15,000 g for 15 minutes. The pellet containing urate oxidase (UO) was redissolved in 10 ml Buffer A (20 mM sodium phosphate, 10 mM imidazole and 0.5 M NaCl at pH 7.4).

A Chelating Sepharose Fast Flow column (Pharmacia) charged with Zn^{2+} was equilibrated with buffer A. The protein solution was loaded onto the column and gently

mixed with the gel. After standing at room temperature for 20 minutes, the column was washed with 7.5 column volumes of buffer A and then 7.5 column volumes of buffer B (20 mM sodium phosphate, 400 mM imidazole and 0.5 M NaCl at pH 7.4). Fractions were assayed for UO spectrophotometrically at 280 nm along with the activity assay described below. Active fractions were pooled and dialyzed against 50 mM Tris pH 8.0, concentrated to ~7 mg/ml using an Amicon concentrator and stored at 4˚C.

Urate Oxidase Assay

The UO activity during purification was monitored spectrophotometrically by measuring the disappearance of urate at its 292 nm absorbance maximum. The standard assay was performed with 980 µl 50 mM Tris pH 8.0 containing 100 µM urate and 20 µl UO sample. This method was used for the determination of activity during purification and to monitor the completeness of UO reactions.

Substrate Synthesis

We have prepared ^{13}C-enriched urate by methods previously reported (Kahn ***et. al***., 1997). This method was used for the synthesis of urate that was ^{13}C-depleted at either position C4 or C5 (Scheme 2-2). For the preparation of urate with ^{13}C-depleted C4, commercially available ^{13}C-depleted cyanide was used as a starting material. To prepare urate with ^{13}C-depleted C4, ^{13}C-depleted bromoacetic acid was used as a starting material for synthesis. ^{13}C-depleted bromoacetic acid was prepared by reacting ^{13}C-depleted acetic acid with N-bromosucciniminde (Zang *et al*, 1998).

Scheme 2-2

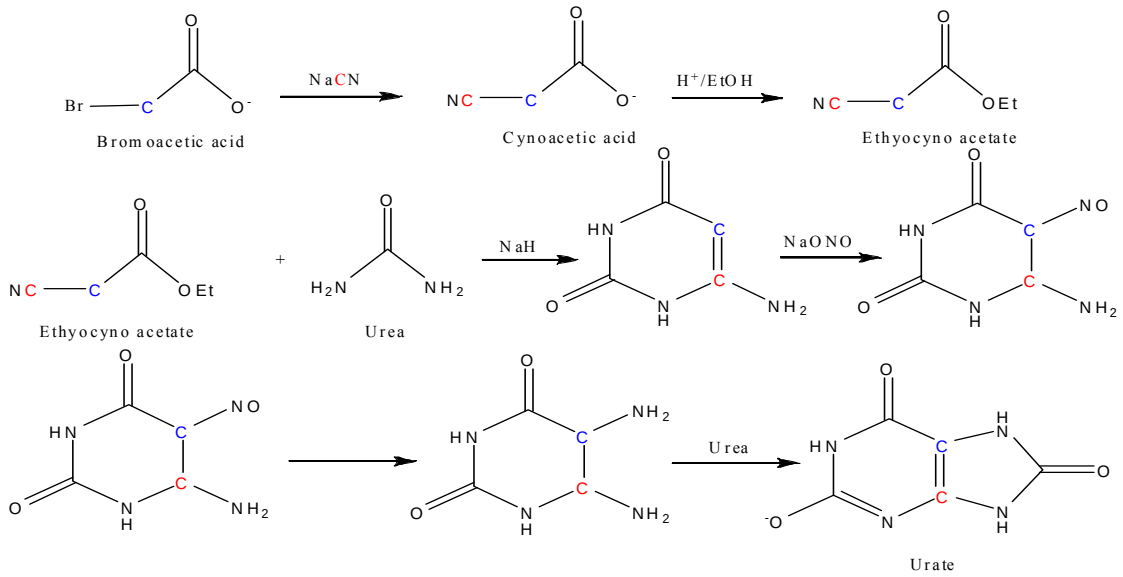

Ferricyanide Assay for determination of Glyoxylate

The ferricyanide assay for glyoxylate was adapted from a previous study (Vogels & Van der Drift, 1970). Each assay consisted of samples to be analyzed, a water blank, and fresh glyoxylate standard solutions. In an eppendorf tube, 125 µl of 0.2M HCl was added to 0.5 ml of sample and heated at 100˚C for 4 minutes. Next, 125 µl of 3 mg/ml phenylhydrazine was added to each of the solutions. The solutions were incubated at 37˚C for 10 minutes for color formation. The solutions were cooled on ice and 0.4 ml concentrated HCl and 125 µl 83 mg/ml potassium ferricyanide solution was added. After incubating at room temperature for 20-30 minutes, the absorbance at 520 nm was used to determine the glyoxylate concentration.

Lactate Dehydrogenase Glyoxylate Assay

Another method used to determine the concentration of glyoxylate in a sample was to monitor the consumption of NADH by a reaction between glyoxylate and lactate dehydrogenase (Scheme 2-3)(LaReau, 1989). First, glyoxylate was dissolved in 5 ml 0.4

M phosphate buffer pH 7.0 and 40 µl 10 mM NADH. The pH was adjusted to 7.0 by the addition of HCl or NaOH as necessary. The solution's absorbance at 340 nm was read before and after the addition of 40 µl 10 mg/ml lactate dehydrogenase. The absorbance was monitored until the reaction had reached completion or for a determined amount of time. The concentration of glyoxylate consumed by the reaction was calculated from the change in absorbance using Beer's Law.

Scheme 2-3

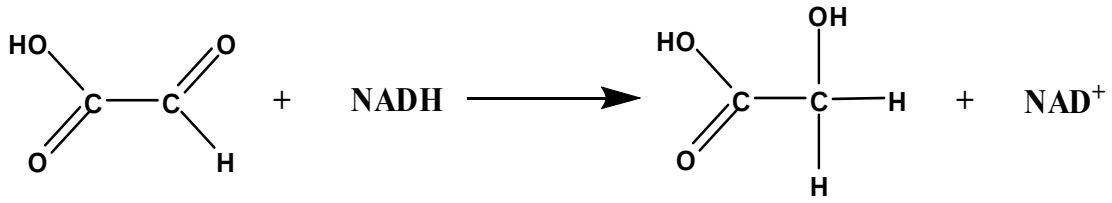

Urea Assay

The urea assay was adapted from a previously reported version (Chaney, 1962). First, two solutions were prepared. Solution A was prepared by mixing 5 grams phenol and 25 mg nitroprusside in 100 ml water. Solution B was prepared by mixing 2.5 grams NaOH along with 4 ml bleach in 100 ml water. Next, 500 µl of solution A and Solution B were added to 500 µl of a fraction sample. The solutions were incubated at 37˚C for 10 minutes. The absorbance at 504 nm of each sample was read to determine whether urea was present.

Isotope Effect Measurement Methods

Method I: Collection of CO_2 for KIE Measurement

For the 100% conversion samples, 2 mM urate in 50 mM Tris buffer pH 8.0 was prepared and divided into six 1.0 ml samples. To each sample, 40 µl 7.17 mg/ml UO was added and reacted overnight at room temperature. The reaction was monitored by mixing 950 µl 50 mM Tris with 50 µl sample and reading the absorbance at 292 nm. After the reaction had reached 100% completion, 2 ml of chloroform was added to extract the enzyme. The water layer from the extraction was loaded onto a Dowex column that had been equilibrated with water. The samples were eluted with 50 ml water followed by 50 ml 0.4 M LiCl. A fraction containing all 50 ml of water was collected and solvent was reduced to 12 ml under reduced pressure. 4 ml of 1.0 M NaOH was added to each 12 ml sample. The sample was heated at 100˚C in an oil bath for 50 min. The samples were removed from heat and 1.4 ml 4.0 M HCl was added. Heat was applied for another 4 minutes at 100˚C to form glyoxylate. The samples were dried under reduced pressure.

Each glyoxylate sample from the KIE reaction was resuspended in 100 ml H_2O and placed in a side arm flask. The samples were then sparged with N_2 for a minimum of 3 hours to remove O_2 from the solution and flask. 100 µl of 10 mM $NaIO_4$ was added to each sample. The valves were sealed and the N_2 was shut off. After 2 hours, 3 ml of concentrated HCl was added to each flask. This resulted in the release of CO_2 from carboxylic acid in the solution. CO_2 from the samples was collected on a vacuum distillation manifold and sent for MS analysis at Paul Cook's laboratory at the University of Oklahoma. The 20% conversion samples were prepared in a similar manner as those of the 100% conversion samples. Six 5 ml samples of 2 mM urate were prepared and

reacted with UO. The reactions were quenched with chloroform when the reaction reached 20% completion as determined by the absorbance at 292 nm.

Method II: Continuous Flow MS KIE

A 10 ml 10 mM urate sample was prepared in 50 mM Tris buffer pH 8.0 and divided into six aliquots. 40 µl 7.7 mg/ml UO was added to each aliquot. The reaction was monitored by mixing 950 µl 50 mM Tris with 50 µl sample and reading the absorbance at 292 nm. After the reaction had reached 100% completion, 2 ml of chloroform was added to extract the enzyme. The water layer containing the reaction product was left to sit overnight for allantoin to form. Next, allantoin was purified on a Dowex column equilibrated with water. After loading the sample, the column was rinsed with 25 ml of water. Allantoin was eluted with 25 ml 0.4 M LiCl. The solvent was removed under reduced pressure. Next, the sample was dissolved in 12 ml of water. To convert the allantoin to allantoate, 4 ml 1.0 M NaOH was added to the sample and heated at 100˚C for 50 minutes. Then, 1.4 ml 4.0 M HCl was added and the reaction was heated at 100˚C an additional 4 minutes. The solvent was removed from the samples under reduced pressure. Each sample was resuspended in 10 mM LiOH and loaded onto a Dowex column equilibrated with 10 mM LiOH. Urea was eluted with 30 ml water followed by glyoxylate being eluted with 30 ml 0.2 M LiCl. 1.0ml concentrated HCl was added to the glyoxylate. The samples were sparged with nitrogen gas for 4 hours and the solvent was removed under reduced pressure.

Similar procedures were used to obtain samples in which UO reactions were stopped at 20% completion. Six 40 ml 8.0 mM urate samples were prepared in 50 mM Tris buffer pH 8.0. 40 µl of 7.7 mg/ml enzyme was added to each sample to initiate the

reactions. The reactions were monitored as mentioned above until the reaction had reached 20% completion. When the reaction reached 20% completion, 2 ml of chloroform was quickly added to extract the enzyme, effectively quenching the reaction. The remaining procedures for the 20% reactions were identical to that of the 100% conversion procedures.

The $^{13}C/^{12}C$ content of the glyoxylate samples was determined by MS analysis. Approximately 42 mg (3 μmol) of each glyoxylate sample was weighed for analysis. The MS analysis was performed by Dr. Cheryl Kelley at the University of Missouri Geology Department.

Method III: Continuous Flow MS KIE (Separation of Allantoin by HPLC)

Samples were prepared as in Method II with the exception of the step in which allantoin was purified. A Shodex Asahipak 7.6 mm ID x 300 mmL HPLC column was equilibrated with 5 mM sodium phosphate buffer pH 4.4. The flow rate was set to 0.5 ml/minute. 100 μl of the reaction mixture was injected onto the column. The allantoin fraction was collected from 12-20 minutes. Injections of the sample were repeated until the entire sample had been purified. The fractions for each reaction mixture were pooled, froze with liquid N_2, and lyophilized to dryness. The remaining steps of the analysis were performed on the pooled samples in the same manner as in Method II for glyoxylate formation and isotopic analysis.

Method IV: Continuous Flow MS KIE (Hydantoinase)

The reaction of allantoin to allantoate by hydantoinase was used for the KIE experiments. Samples were prepared according to Method II with the exception of the allantoin separation and the allantoin reaction to glyoxylate. After the UO reaction was

complete, 200 µl 10 mg/ml hydantoinase prepared in 20 mM phosphate buffer pH 7.5 was added to each reaction mixture. The reactions were incubated overnight at room temperature so that the allantoin to allantoate reaction would reach completion. 200 µl chloroform was added to extract the enzyme. To the water layer, 325 µl 0.15 M HCl was added and the solution was incubated at 100˚C for 12 minutes. Glyoxylate was purified and analyzed as in Method II.

Method V: O_2 Concentration Effects on the C4-C5 KIE and O_2 KIE

To measure the effect of O_2 concentration on the C4-C5 KIE of urate in the UO reaction, solutions were prepared for a 20% KIE reaction as in Method II. Each solution was placed in a side arm flask and sparged with 5, 10, or 100% O_2 for 1 hour. UO was added to each solution. Reactions were carried out under the oxygen atmosphere until the reaction reached 20% completion. These partial completion reactions were compared to the 100% reactions measured using Method II to determine the KIE. Similarly, ^{18}(V/K) KIE was determined by collecting the allantoin produced from the reactions. This allantoin was dried and analyzed by MS to determine the $^{18}O/^{16}O$ ratio.

Determination of Water Content

Thermogravimetric (TGA) analysis was performed using a TA instruments Q50 TGA. Approximately 2 mg of sample was placed in a tared cup on the instrument. In the ramp setting, the sample was heated at a rate of 15.00 degrees/minute from room temperature to 150˚C. Results obtained were reported as % Weight vs. Temperature.

Calculation of KIE from MS data

The ^{13}(V/K) KIE was calculated from the MS data. First, the $Ratio_{sample}$ was calculated from the MS data. The variation in isotope ratios from the international standard is defined by the following equation:

$$\delta = \left(\frac{Ratio_{sample}}{Ratio_{PBD-std}} - 1 \right) \times 1000 \qquad (2\text{-}1)$$

Where δ is the value measured by MS and $Ratio_{PBD\text{-}std}$ is the universal standard value, 11237.2±9.0 x 10^{-6} for $^{13}C/^{12}C$ (J. Hayes, 1982). Next, the ^{13}(V/K) for each of the 20% completion reactions was calculated using Equation 2-2 (Cleland, 1987).

$$^{13}(V/K) = \frac{\log(1-f)}{\log\left[1 - \frac{f \times (low\_conversion)}{(high\_conversion)}\right]} \qquad (2\text{-}2)$$

Where *f* is the percent completion of the reaction as determined by UV-spectroscopy, low_conversion is the $Ratio_{sample}$ of the 20% reaction, and high_conversion is the average $Ratio_{sample}$ value for the six 100% completion reactions.

The ^{18}(V/K) KIE was determined using the same equations, But $Ratio_{SMOW\text{-}std}$ was used in place of $Ratio_{PBD\text{-}std}$ with a value of 2005.20±0.43 x 10^{-6} (Hoefs, 1997).

UV Spectroscopy

UV analysis was performed on a Cary 50 Bio UV-spectrophotometer.

2.3 Results

In order to measure the KIE of UO at the C4 and C5 positions of urate, a method to isolate the carbon from these positions for MS determination of its $^{13}C/^{12}C$ content was developed. By reacting urate with UO, the short lived product, 5-hydroxyisourate, was formed (Scheme 1-1). This product degrades to allantoin with a half-life of 30 minutes. Therefore, a method in which allantoin collected from the UO reaction is degraded to glyoxylate containing carbons originating from the C4 and C5 positions is crucial in the KIE analysis of UO.

To separate allantoin from urate, a Dowex anion exchange column was chosen. Allantoin and urate have a large difference in their pKa values of 8.6 and 5.8 respectively (Kahn, 1997). Because of this difference in pKa, at a pH of 7.0 allantoin should be neutral and flow through the column while urate would be negatively charged and bind to the column. By lowering the pH below 5.8 with a lithium chloride mobile phase, urate should be released from the column. The elution time of urate was determined by its absorbance at 292 nm in fractions collected from the column. The elution point of allantoin was determined by differential glyoxylate analysis (Vogel & Van der Drift, 1970). A 2 mL mixture of 5 mM urate and 5 mM allantoin sample was loaded onto the column and eluted at ~1 ml/minute with a stepwise gradient of LiCl (0.0, 0.2, 0.4, 0.6, and 0.8 M). Allantoin eluted with the water fraction and the urate was eluted with 0.4 M LiCl (Figure 2-1).

Vogels and Van der Drift have developed a reaction to form glyoxylate from allantoin (Vogel & Van der Drift, 1970). This reaction was used to develop a procedure to isolate glyoxylate containing carbons originating from the C4 and C5 positions of urate. In this

procedure, allantoin was reacted with NaOH and heated to 100˚C to form allantoate. Second, HCl was added to the reaction mixture and heated at 100˚C until glyoxylate and urea were formed. To insure that there was no isotopic fractionation resulting from the reaction, the reaction must go to 100% completion. To optimize the reaction for the 100% conversion of allantoin to glyoxylate, product formation was analyzed. The reactions consisted of 1 ml samples of 30 mM allantoin, 2 ml H_2O, and 1 ml 0.5 M NaOH. The reaction mixture was then heated to 100˚C. After 8 minutes, the reaction mixture was removed from heat and 1 ml 0.65 M HCl was added. The reaction mixture was heated at 100˚C for another 4 min. After cooling, lactate dehydrogenase was added. The amount of glyoxylate formed was determined by measuring the NADH consumed by lactate dehydrogenase (Scheme 2-3). The ferricyanide assay and ^{1}H NMR spectroscopy were also used to monitor the reaction of allantoin to glyoxylate. The parameters of the optimized reaction for the 12 ml of allantoin recovered from the UO reaction was to add 4 ml of 1.0 M NaOH to the reaction mixture and heat at 100˚C for 50 min. The reaction mixture was removed from heat and 1.4 ml 4.0 M HCl was added. The reaction mixture was heated an additional 4 minutes at 100˚C whereupon glyoxylate was formed.

Figure 2-1: Separation of urate and allantoin on a Dowex column. The absorbance of urate at 292 nm is shown in red. The allantoin assay measured at 520 nm is shown in green.

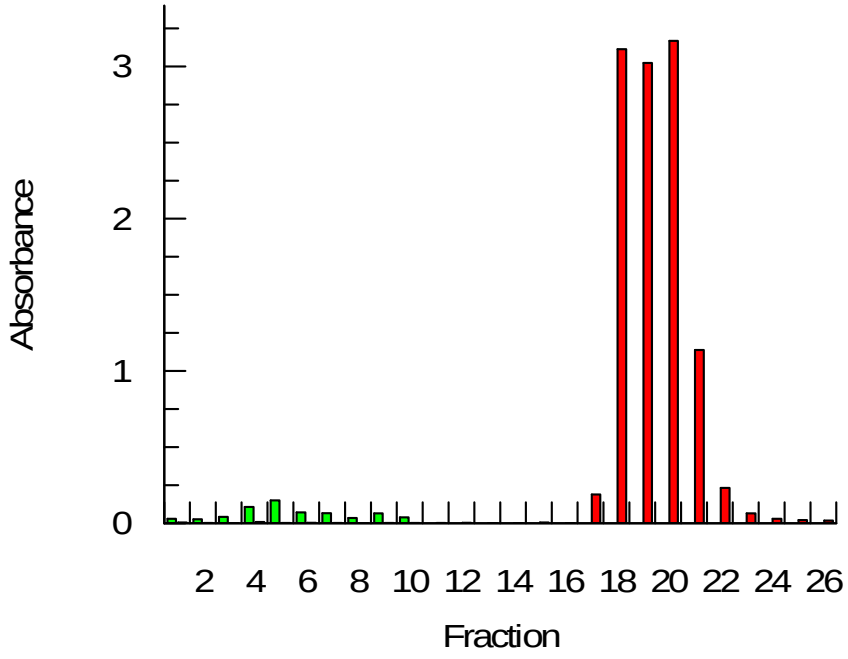

In order to determine the $^{13}C/^{12}C$ ratio of a single position by MS, the glyoxylate isolated from KIE reactions needed to be collected as CO_2. To isolate CO_2 originating from the C5 position of the urate, a reaction of glyoxylate with $NaIO_4$ to form formic acid and CO_2 was used (Scheme 2-4). The optimized reaction conditions were as follows. 200 μM glyoxylate in D_2O was mixed with 0.0535 g $NaIO_4$ and incubated at room temperature for 1 hour. The reaction completion was determined by comparing ^{13}C NMR spectra before and after the addition of $NaIO_4$. In the first spectra acquired, two peaks were observed at 173.298 ppm and 88.275 ppm (Figure 2-2A). After the reaction had reached completion, only one peak was observed at 166.197 ppm (Figure 2-2B). This is consistent with two carbons from glyoxylate in the hydrate form being converted to formic acid and CO_2. The CO_2 evidentially escaped from the solution as gas.

Scheme 2-4

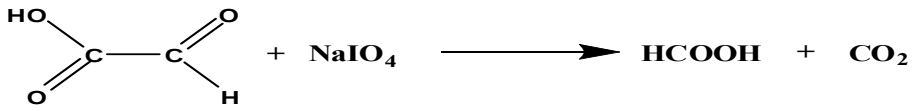

Figure 2-2: ^{13}C NMR spectra of glyoxylate reaction before (A) and after (B) the reaction with $NaIO_4$. The peak at 66.66 ppm if from the dioxane standard.

(A)

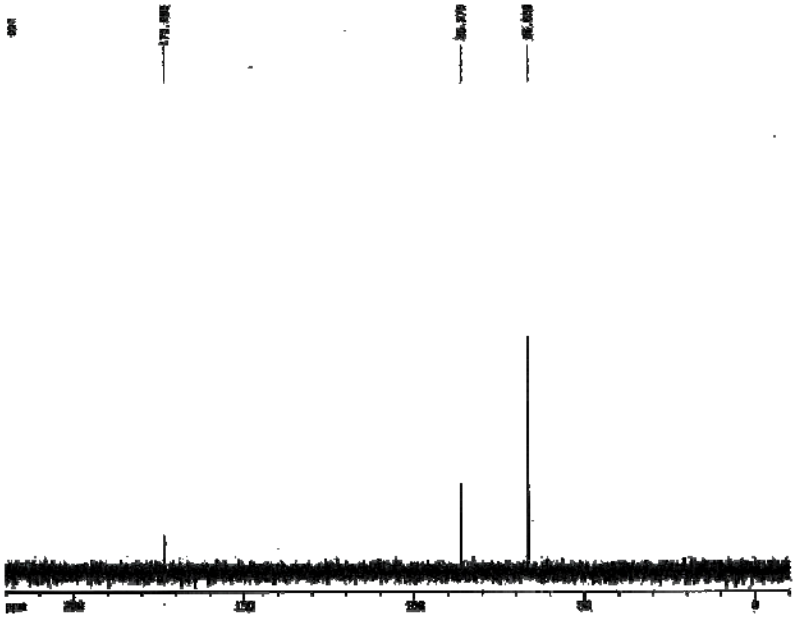

(B)

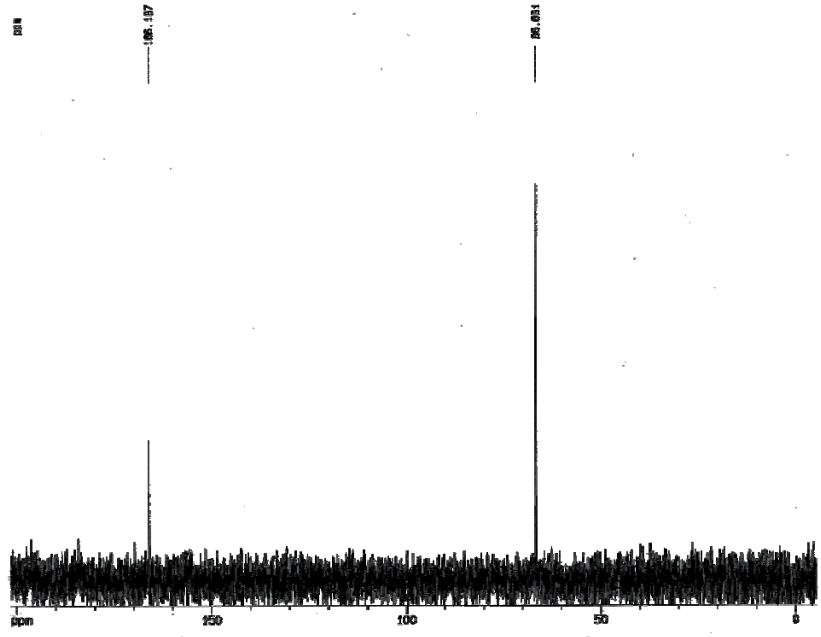

Method I: CO_2 isolation for C5 KIE determination.

Glyoxylate from six 100% and six 20% UO reactions were prepared as in Method I. The glyoxylate samples obtained from the KIE reactions were placed in sealed side arm flasks and reacted with $NaIO_4$ to form formic acid and CO_2. The CO_2 from this reaction, which originated from the C5 position of urate, was collected on a vacuum distillation manifold. The collected CO_2 was analyzed by isotope ratio mass spectroscopy in Paul Cook's laboratory at the University of Oklahoma. No CO_2 was present in the reaction products. Because access to the MS facility in Oklahoma was not convenient, a new direction was taken.

Method II: Continuous Flow Development

More convenient access to a continuous flow MS, by collaboration with Cheryl Kelley at the University of Missouri-Columbia, changed the direction of the KIE measurement. Continuous flow MS can measure the isotopic ratio of solid samples instead of CO_2. Therefore, a method of isolating glyoxylate from the KIE reactions for MS was needed.

The first part of the method in which urate is reacted to form glyoxylate was the same as in Method I. For continuous flow MS analysis, glyoxylate needed to be separated from urea. Glyoxylate was separated from urea on a Dowex column. First, 100 mM of urea and 100 mM glyoxylate were dissolved in water to make a standard. The column was equilibrated with water and then 1 ml of standard was loaded onto the column. A step-wise gradient of 0.000, 0.025, 0.05, 0.075, 0.10, 0.15 and 1.0 M LiCl in 30 mL increments was used to determine the elution point of the glyoxylate and urea. Glyoxylate was found in the 0.000, 0.025, 0.050, and 0.075 M LiCl fractions. This was determined

by the lactate dehydrogenase assay. Since the column didn't bind 100% of the glyoxylate, this method was abandoned.

In the next investigation, a Dowex column was equilibrated with 10 mM LiOH. First, a standard of 100 mM glyoxylate and 100 mM urea was prepared in 10 M LiOH. Second, 1 mL of this standard was loaded onto the column. The standard was eluted with 126 mL 10 mM LiOH followed by 100 mL 1M HCl. 7 ml fractions were collected. Third, fractions were adjusted to pH 6-8 with NaOH or HCl solutions as necessary. Fourth, these fractions were assayed for the presence of urea and glyoxylate by the urea and lactate dehydrogenase assays. This separation is shown in Figure 2-3. Only a small amount of glyoxylate was eluted from the column, which made it difficult to collect and measure a sample for MS analysis. Therefore, LiCl was used in place of HCl for preparation of the mobile phase. This increased the amount of sample after drying, which allowed glyoxylate to be collected and weighed.

Figure 2-3: Separation of glyoxylate from urea. The urea assay was measured at 504 nm (red). The lactate dehydrogenase assay measured at 340 nm was used to determine the glyoxylate concentration (black). The mobile phase gradient is represented by the dashed line.

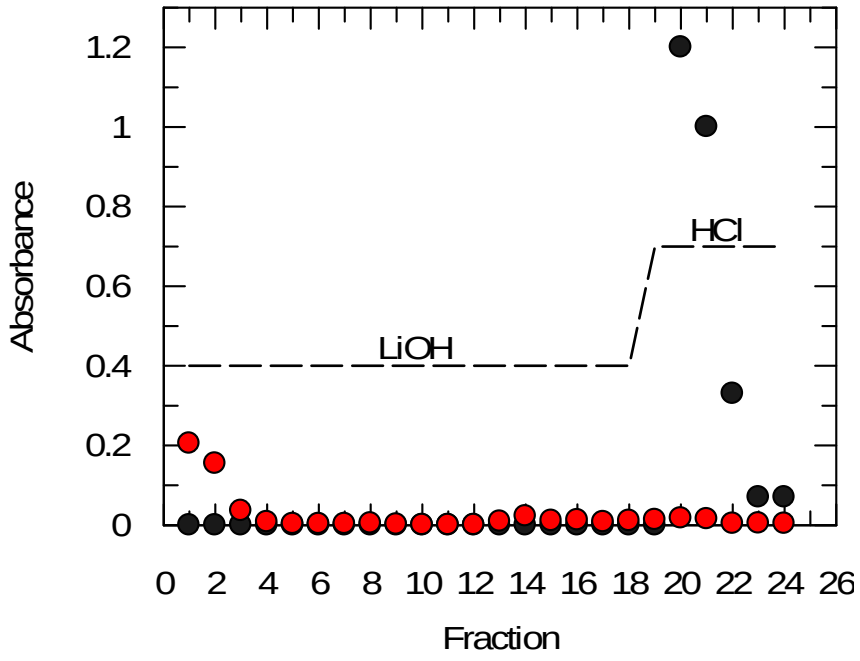

The concentration of glyoxylate from samples of authentic glyoxylate, authentic glyoxylate purified on a Dowex column, and glyoxylate that was isolated from a reaction of allantoin were compared using the ferricyanide assay. It was determined that the amount of glyoxylate from the allantoin reaction was less than expected. Therefore, not all of the allantoin from the UO reaction was being converted to glyoxylate. To investigate which step of the reaction was not going to completion, the allantoin to allantoate and allantoate to glyoxylate half-reactions were analyzed.

For the optimization of allantoate to glyoxylate, 0, 1.0, 2.0, 3.0, 4.0, and 5.0 mM allantoate samples were prepared. To each 1.5 ml allantoate sample, 50 µl of HCl was added. The samples were then heated at 100˚C for 4 min. The amount of glyoxylate produced from the reaction was determined by analyzing 0.5 ml of each sample by the ferricyanide assay and comparing to a standard curve of glyoxylate (Figure 2-4). The allantoate to glyoxylate reaction was shown to go to completion. Therefore, it was determined that the allantoin to allantoate half-reaction was responsible for the lack of glyoxylate formation.

Figure 2-4: Allantoate to glyoxylate reaction (green) compared to the standard curve (red).

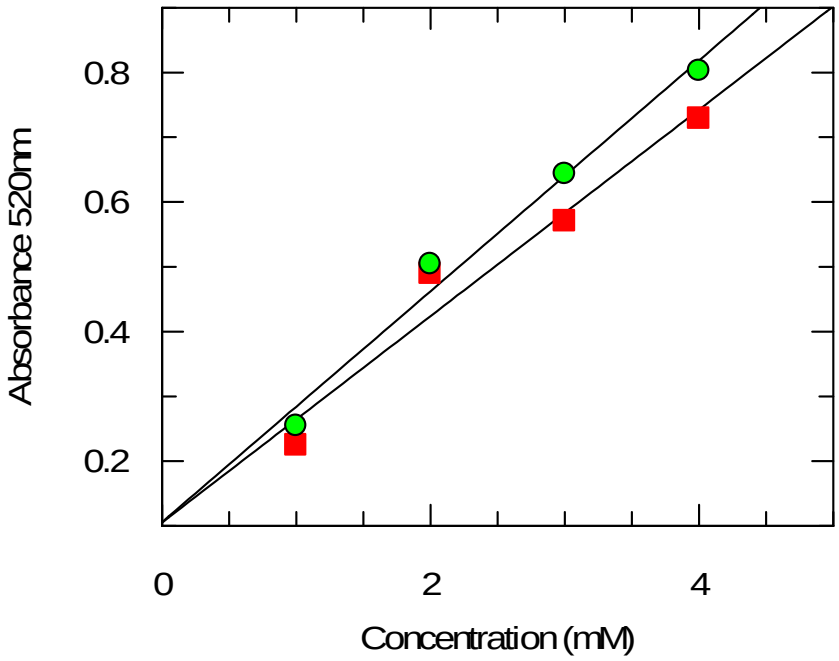

To investigate whether reaction time was the limiting factor in the allantoin to allantoate reaction, the reaction time of allantoin with NaOH was stopped at 30, 40, 50, 60, and 70 minutes. Glyoxylate formation increased with time, but the reaction did not reach completion. Next, the amount of NaOH used in the reaction was increased from 0.5 M to 1.0 M. Allantoin samples were reacted for 40, 50, 60 and 80 minutes, and then analyzed as above. An increase in allantoin concentration was observed, but the reaction did not reach completion (Figure 2-5). The next variable that was analyzed was the amount of HCl used in the reaction. The amount of 0.4 M HCl was increased from 100 to 150 µl. When glyoxylate concentrations for these reactions were compared to a standard curve of glyoxylate, it was observed that all the reactions had reached completion (Figure 2-6). Varying the sample heating time didn't affect the formation of glyoxylate even with higher HCl concentration. To expand on this, reaction products produced from solutions of 1.0, 2.0, 3.0, 4.0, and 5.0 mM of allantoin were compared to a standard curve (Figure 2-7). From this data, it was shown that the reaction completion was determined by the amount of HCl. To determine whether glyoxylate was lost upon purification, MS analysis of column purified glyoxylate and non-purified glyoxylate were compared (Table 2-1). Both glyoxylate samples had the same calculated ratio sample of 0.0110. This result indicates that glyoxylate was not lost in the purification step and that the loss of glyoxylate was due to the reaction of allantoin to allantoate.

Table 2-1: MS analysis of glyoxylate eluted from a Dowex column

Sample	δ	Ratio Sample
Glyoxylate	-23.04	0.01098
Glyoxylate	-23.15	0.01098
Glyoxylate from column	-21.76	0.01099
Glyoxylate from column	-20.99	0.01100

Figure 2-5: The effect of increasing the NaOH concentration in the reaction of allantoin to glyoxylate.

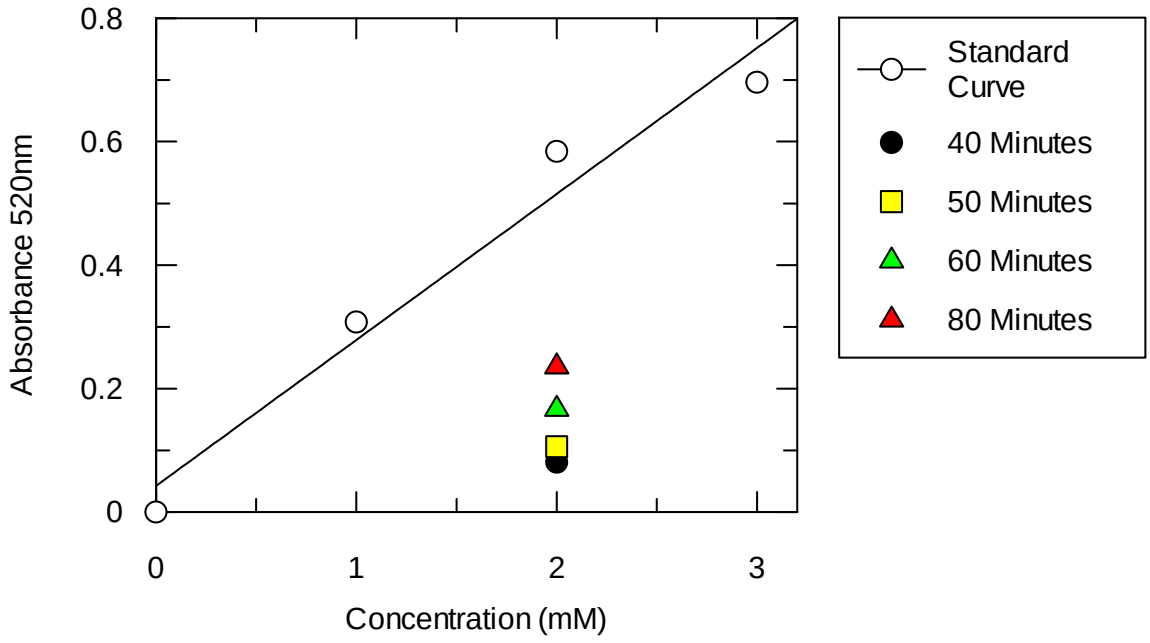

Figure 2-6: Increasing the concentration of HCl in the reaction of allantoin to glyoxylate allowed the reaction to reach completion for all reaction times.

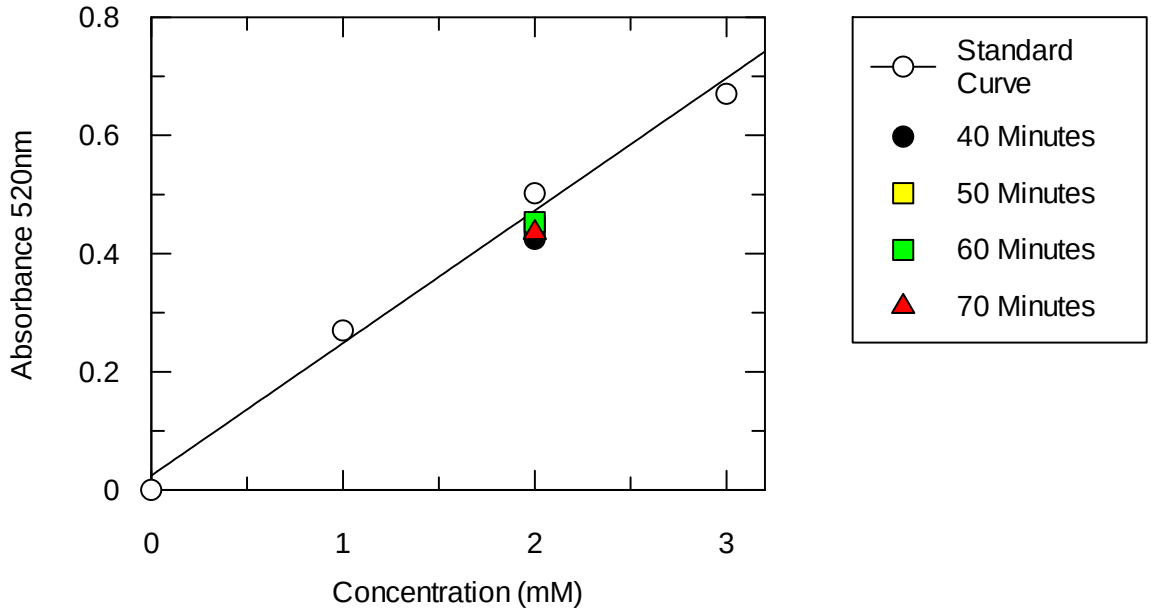

Figure 2-7: Allantoin to glyoxylate reactions of 1.0, 2.0, 3.0, 4.0, and 5.0 mM allantoin solutions were compared to a standard curve of glyoxylate.

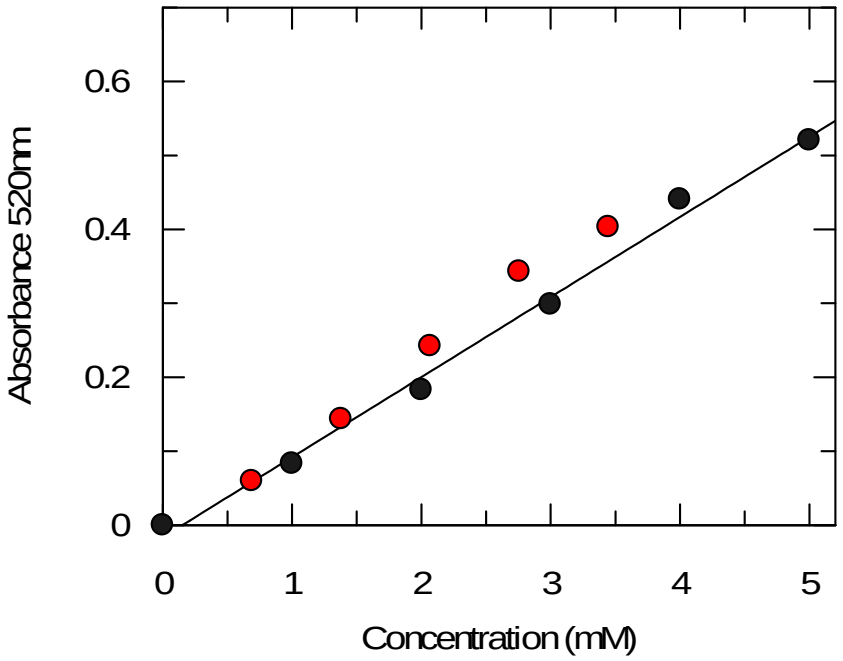

Method II: Continuous Flow KIE Measurement

With Method II optimized for the measurement of ^{13}(V/K) KIE at positions C4 and C5 of urate, we were ready to prepare samples for KIE determination. For the 20% completion reactions, six 1 ml 10 mM urate samples were prepared in 50 mM Tris buffer pH 8.0. To initiate the reactions, 80 µl 2.0 mg/ml UO was added to each sample. Five 40 ml samples of 8.0 mM urate were prepared and 40 µl of enzyme was added to start the reaction. Approximately 42 mg (3 µmol) of glyoxylate from each sample was analyzed by MS to determine the $^{13}C/^{12}C$ content, δ (Table 2-2). A C4-C5 ^{13}(V/K) KIE of 1.0045±0.0012 was calculated by comparing the reactions run to 100% and 20% completion.

Table 2-2: $^{13}C/^{12}C$ content of glyoxylate samples prepared for KIE

Sample (Completion)	δ	Ratio Sample	^{13}(V/K)
1 (20%)	-23.901	0.010969	1.0013
2 (20%)	-25.798	0.010947	1.0036
3 (20%)	-27.888	0.010924	1.0059
4 (20%)	-26.041	0.010944	1.0038
5 (20%)	-29.681	0.010904	1.0078
1 (100%)	-30.502	0.010894	NA
2 (100%)	-20.104	0.011011	NA
3 (100%)	-21.952	0.010990	NA
4 (100%)	-18.983	0.011024	NA
5 (100%)	-23.997	0.010968	NA
6 (100%)	-20.668	0.011005	NA

To determine the intrinsic isotope effect of the UO reaction, the ^{13}(V/K) KIE at various concentrations of the oxygen substrate was measured. The C4-C5 KIE of urate in the UO was measured under different concentrations of O_2. Twelve reaction mixtures were prepared in the same manner as the 20% KIE reactions above. Six of these reaction

mixtures were placed in side arm flasks and sparged for one hour with gas containing 10% O_2. The other six reaction mixtures were sparged with gas containing 100% O_2. UO was added to each mixture and the reactions were carried out at the specific oxygen concentration until reaching 20% completion. For the calculation of the KIE of for these reactions, previously determined values from the 100% completion reactions were used. The ^{13}(V/K) KIE with 10% and 100% O_2 were 0.9981±0.008 and 0.9955±0.0027 respectively. Since the KIE at 10% and 100% O_2 are essentially the same, the intrinsic isotope effect was not able to be determined with this method.

Another method used to determine the intrinsic isotope effect on the UO reaction mechanism was by measuring the ^{18}(V/K) KIE. UO mixtures were reacted to 20% as above, under oxygen atmospheres of 5%, 20%, and 100%. Instead of degrading the product to glyoxylate, allantoin was collected. Allantoin samples were analyzed by MS for their oxygen isotopic composition. 100% conversion reactions of urate to allantoin were also conducted under atmospheric conditions. The results are tabulated below in Table 2-3. Figure 2-8 shows the trend of the data. A fourth ^{18}(V/K) KIE measurement was made for samples at 10% oxygen concentration. These samples along with the previous samples were analyzed by MS. It was found that the oxygen content had increased in the previous samples after being in the desiccator for ~5 days (Table 2-3).

Table 2-3: Results for O_2 KIE under different atmospheric conditions.

Sample	^{18}(V/K)	Repeated ^{18}(V/K)
5% O_2	0.91662	0.876845
10% O_2	NA	0.869744
20% O_2	0.922198	0.888912
100% O_2	0.931399	0.973425

Figure 2-8: The effect of oxygen concentration on ^{18}(V/K) KIE.

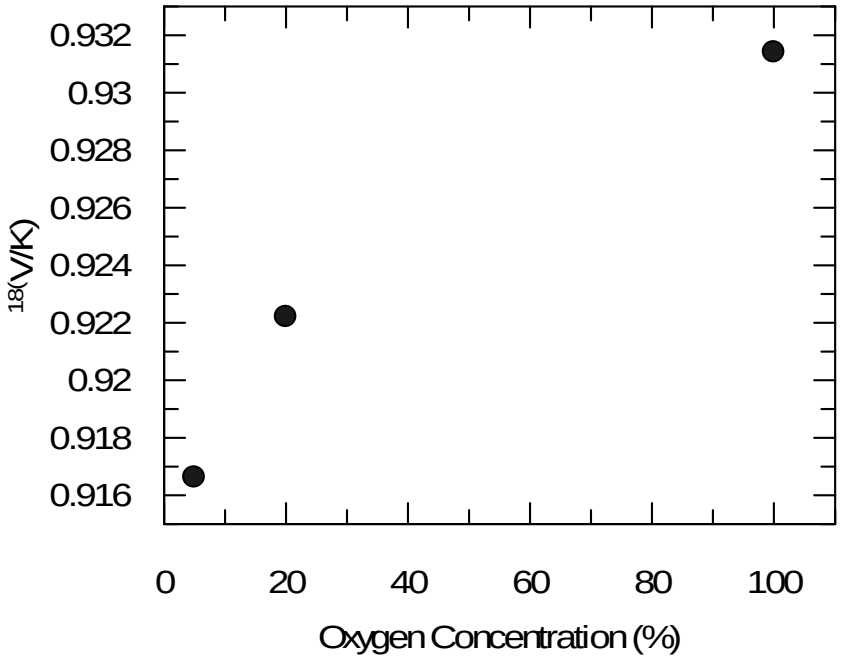

To determine whether water was being absorbed by the samples, TGA (thermal gradient analysis) was used to analyze the water content of the samples. It was found that ~18% of the sample weight was water. Elution of samples by LiCl, NaOH and KCl gave water content values of 9.3, 16.9, and 1.3%. Therefore, KCl was used to elute the samples. The sample eluent was placed in a vacuum desiccator for 3 days to reduce the water content to 0.7%. To reduce the volume of salt in the sample, a mixture of 0.4 M HCl and 13.4 mM KCl was used to elute the allantoin. The ^{18}(V/K) KIE experiments were repeated eluting glyoxylate with the KCl/HCl solution. The results can be found in Table 2-4 and Figure 2-9. The ^{18}(V/K) values obtained were quite similar under each oxygen condition. The ^{18}(V/K) value was expected to approach 1.0 as oxygen concentration increases. Since this was not observed, it was possible that not all the water was being removed from the sample or water was absorbed by the sample before being loaded onto the MS.

Table 2-4: Effect of O_2 Concentration on Oxygen KIE

Sample	^{18}(V/K)	Error
10% O_2	1.0304	0.0034
20% O_2	1.0317	0.0052
100% O_2	1.0362	0.0033

Using Method II, the C4-C5 KIE experiments were repeated with urate that was ^{12}C-labled at the C4 position. A ^{13}(V/K) KIE of 0.9323±0.0097 was measured. The ^{13}C vs. VPDB values from the ^{12}C-labeled substrate were expected to be approximately -400, since 50% of the carbon in glyoxylate was ^{12}C. The value was actually measured to be in

the range of -100 to -159. This result indicated that there was more ^{13}C present than what was expected.

Figure 2-9: The effect of oxygen concentration on ^{18}(V/K) KIE.

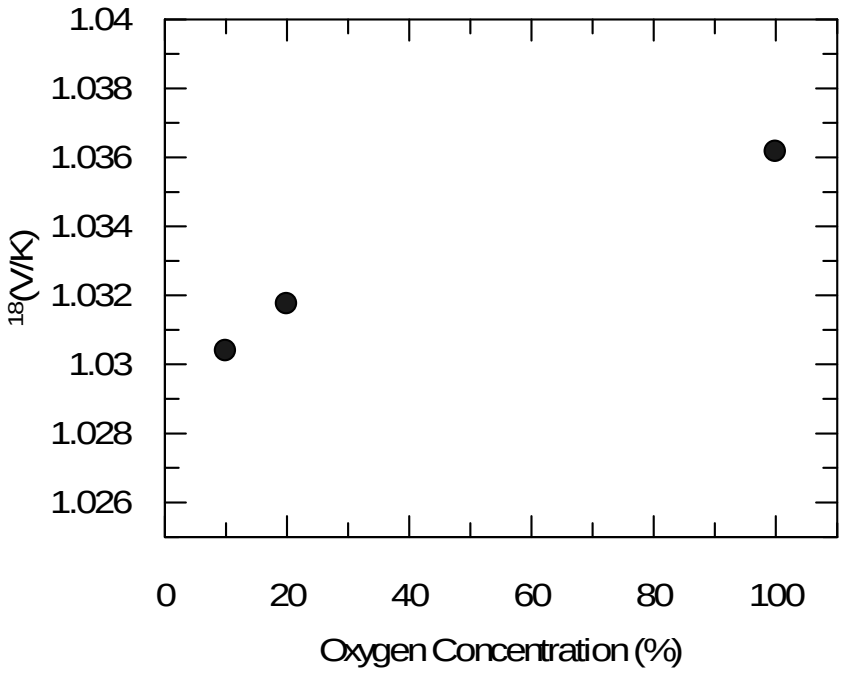

To study the reason behind the loss in ^{12}C content, KIE reactions were performed with ^{12}C-labeled urate. The resulting allantoin and glyoxylate were collected and analyzed by MS along with the ^{12}C-labeled urate. The δ values for urate, allantoin, and glyoxylate were found to be -229, -53, and -35 respectively. The measured δ value of the ^{12}C-labeled urate indicated that it didn't contain any contamination. For the allantoin and glyoxylate samples, the expected δ values were -300 and -400 respectively. From this data it was obvious that a large increase in ^{13}C occurred when allantoin was isolated. It was possible that a smaller increase in ^{13}C occurred when glyoxylate was isolated.

Method III

The steps of the urate to allantoin portion of Method II were analyzed to determine when ^{13}C contamination was introduced into the allantoin samples. Urate to allantoin reactions were prepared in both 50 mM Tris and phosphate buffers. Samples were collected at the following times: before extraction, after extraction, and after column purification (Table 2-5). From this, it was determined that 50% of allantoin was lost on the column. Therefore, a HPLC method was developed to separate allantoin from urate. A Shodex column was first equilibrated with 5 mM $NaPHO_4$ pH 4.4. Next, samples of 10mM urate and 10mM allantoin were prepared along with a sample containing 10mM of each. Samples of allantoin and urate were injected onto the HPLC to determine their retention times. Next, the mixture was injected to determine the resolution between urate and allantoin (Figure 2-10). Collected fractions were assayed by the ferricyanide assay to determine the amount of allantoin collected. It was determined that 100% of the allantoin eluted between 11-22 minutes.

Table 2-5: Concentration of allantoin in samples		
Time	Sample	Concentration (μM)
Before Extraction	T-1	203
	T-2	204
After Extraction	T-1	205
	T-2	205
After Column Purification	T-1	104
	T-2	93
Before Extraction	P-1	194
	P-2	194
After Extraction	P-1	202
	P-2	203
After Column Purification	P-1	91
	P-2	91

KIE experiments were repeated using the HPLC method of the allantoin separation. A ^{13}(V/K) value of 1.000±0.004 was determined from these experiments. When the 100% completion reactions were performed with ^{13}C4-depleted urate, glyoxylate was not as ^{13}C depleted as was expected. Therefore, it was hypothesized that carbon was being introduced into the reaction. When glyoxylate samples from the ^{12}C4 reactions were analyzed by ^{1}H NMR (Figure 2-11), it was obvious that impurities had been introduced.

Figure 2-10: Resolution of allantoin and urate by HPLC.

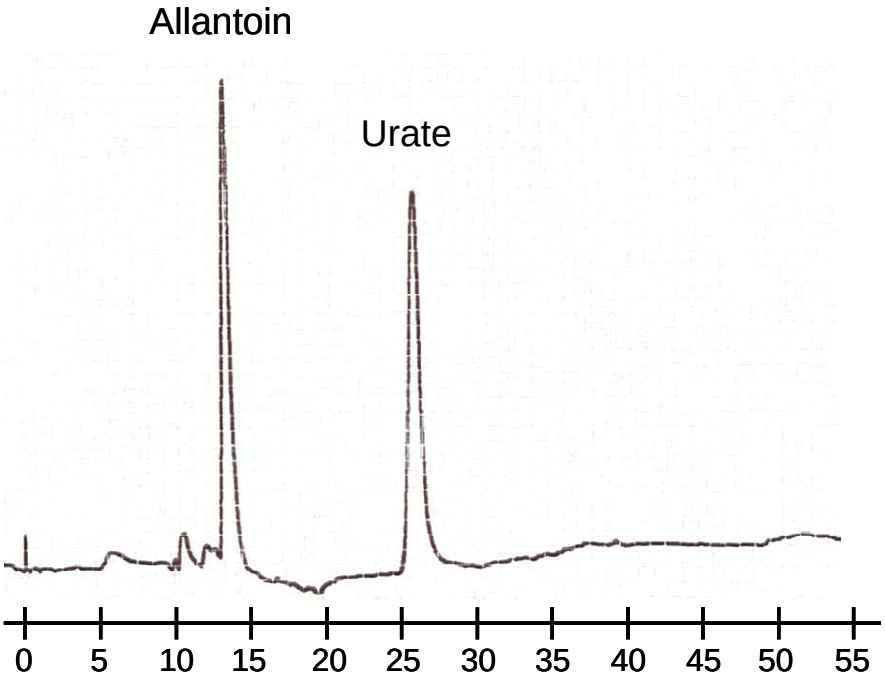

Figure 2-11: ^{1}H NMR of glyoxylate from ^{12}C samples.

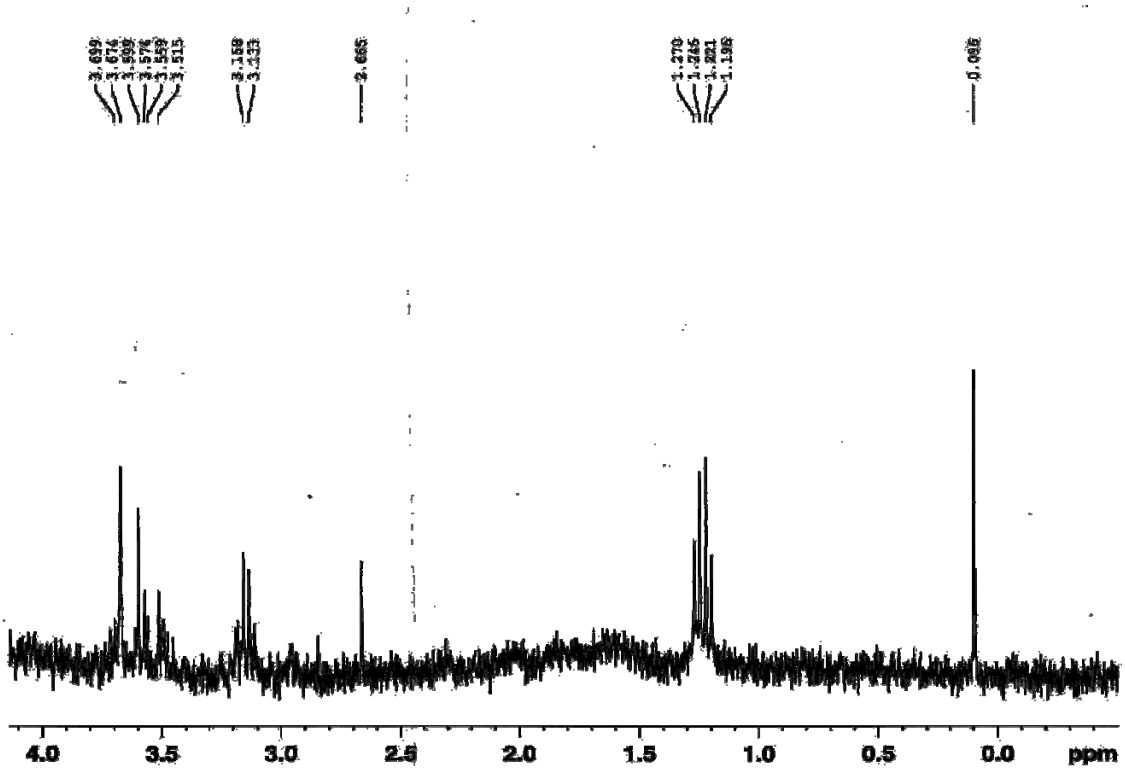

Method IV

Although purification of allantoin by HPLC was effective, it was time and labor intensive. Using hydantoinase to catalyze the reaction from allantoin to allantoate was found to save time. Since hydantoinase reacts specifically with allantoin and not urate, column purification of allantoin was not necessary. With this purification step eliminated, we hoped to increase the purity of glyoxylate in the KIE measurements. When 200 µl of 10 mg/ml hydantoinase was added to 800 µl 10 mM of allantoin, the reaction went to completion. Allantoate was analyzed with an abbreviated ferricyanide assay. Method IV was used to form glyoxylate from 10 mM of allantoin. The product was analyzed by ^{1}H NMR for purity (Figure 2-12). One significant impurity was found at 3.6 ppm. To further investigate the source of the impurity, the LiOH and LiOH fractions of the glyoxylate separation were analyzed by ^{1}H NMR. No impurity or glyoxylate peaks were observed in the LiOH fraction. Tris and sodium phosphate buffers were also analyzed by ^{1}H NMR. The observed impurity was found in the Tris spectrum at 3.6 ppm. Since the $NaPHO_4$ did not contain this impurity, the reaction of allantoin to glyoxylate was repeated using phosphate buffer. No impurity was observed in the glyoxylate product when the reaction was carried out in phosphate buffer (Figure 2-13).

The C4-C5 KIE was measured again using Method IV. A value of 0.9967±0.0002 was determined for the C4-C5 KIE. When ^{13}C-depleted urate samples were analyzed by testing the 100% reaction, the ^{12}C content of the samples was closer to the predicted value, but these samples still contained a higher concentration of ^{13}C than expected. The ^{13}C vs. PDBV values of these samples were between -147 and -193 (about half of the expected value).

Figure 2-12: ^{1}H NMR of glyoxylate isolated from reaction. An impurity was identified at 3.6 ppm.

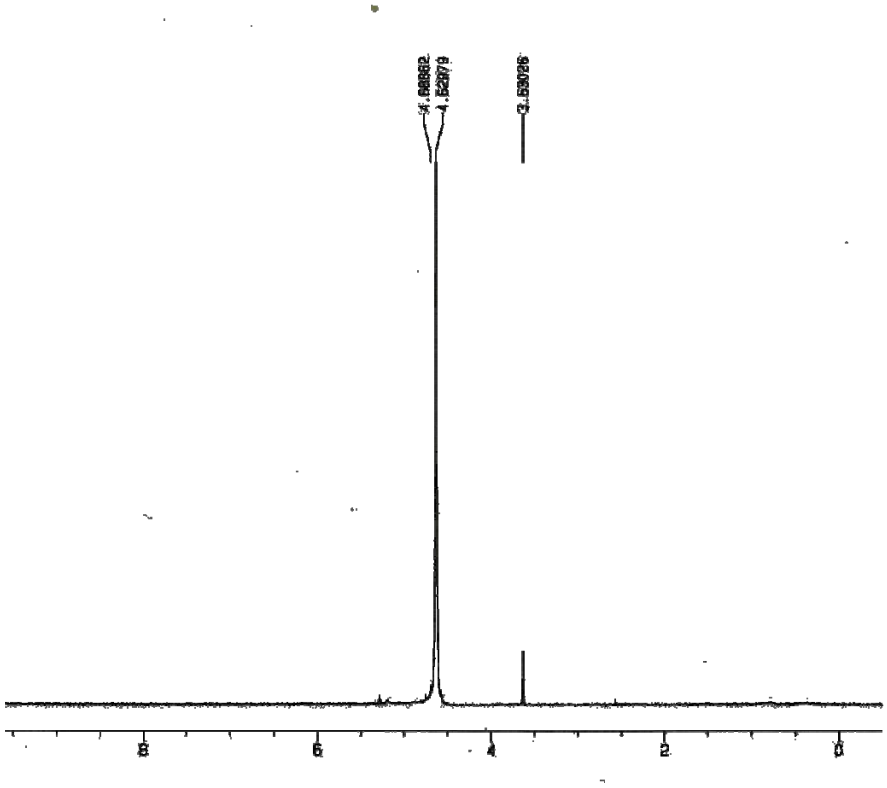

Figure 2-13: Glyoxylate isolated from reaction performed in phosphate buffer. There is no impurity at 3.6 ppm.

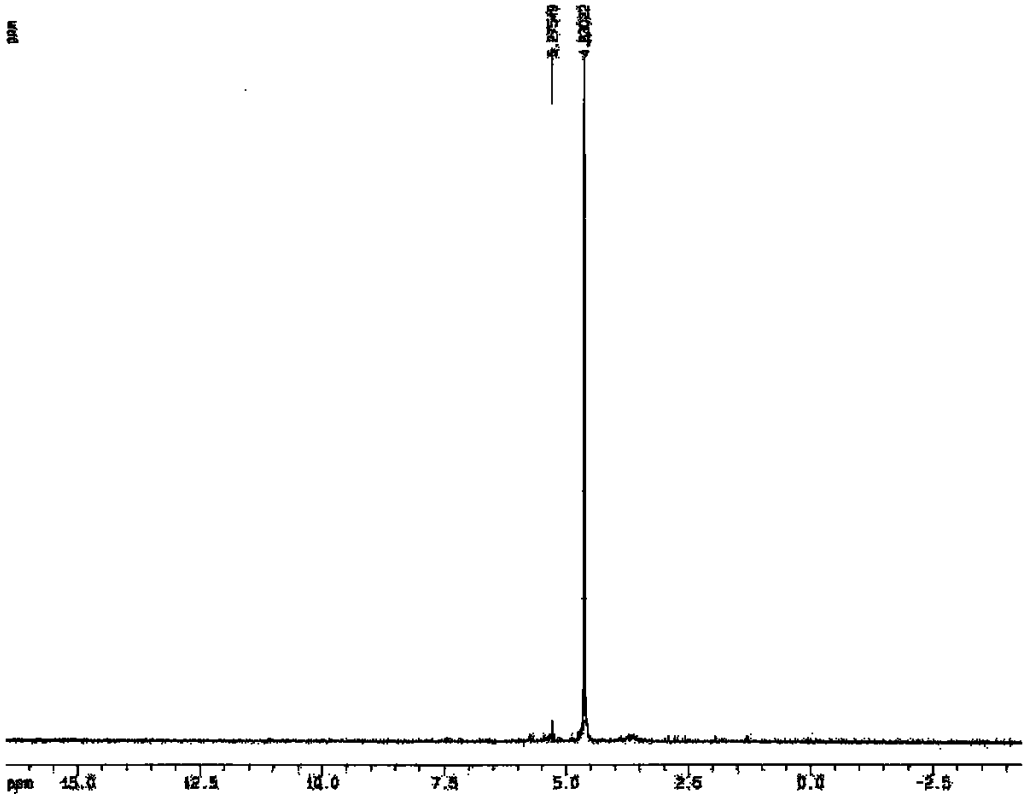

2.4 Discussion

We explored several techniques of measuring the C4-C5 KIE of urate arising from the urate oxidase reaction. The competitive method was the basis for the KIE measurements, in which the $^{13}C/^{12}C$ content at a single position of the substrate and products were compared (O'Leary, 1980). Since urate and the product of the UO reaction, allantoin, contain five carbons, a method of measuring the isotopic ratio at a position of interest was devised. In Method I, we attempted to measure the $^{13}C/^{12}C$ content at position C5 by isolating allantoin. After isolating allantoin, it was degraded to glyoxylate. Glyoxylate contained two carbons that originated from the C4 and C5 positions of urate. By reacting glyoxylate with $NaIO_4$, C5 containing CO_2 was formed. The CO_2 was collected and then analyzed by MS, but there was not enough CO_2 collected to measure the $^{13}C/^{12}C$ content. Since there was a more convenient access to a continuous flow MS at the University of Missouri, this method was abandoned.

Continuous flow MS had not previously been used for measuring KIE. Therefore, novel techniques for measuring the KIE of complex molecules were explored. A continuous flow MS can accurately measure the isotopic ratio of carbon in a solid sample. This eradicated the need to convert glyoxylate to CO_2. Before analyzing whole molecules, a new technique was devised which utilized ^{13}C-depletion of all carbons that are not of interest. Urate was synthesized with ^{13}C-depleted carbon at the C4 or C5 position. When the ^{13}C-depleted substrate was degraded to glyoxylate, the measurement of the ^{13}C KIE at the non-labeled carbon was possible. This selective ^{13}C-depletion allows KIE determination at a single carbon of interest in multiple carbon containing molecules. This new method of measuring the $^{13}C/^{12}C$ content by continuous flow MS

allowed for the measurement of whole molecule isotopic content measurement as opposed to isolating a single carbon containing molecule.

Method II was used to measure the C4-C5 KIE by utilizing continuous flow MS. Initially, urate was degraded to allantoin. Allantoin was then reacted to form glyoxylate (Scheme 1-2). Glyoxylate was purified on a Dowex column for MS analysis. The $^{13}C/^{12}C$ isotopic ratio at position C4 and C5 of allantoin were analyzed. A $^{13}(V/K)$ KIE value of 1.0045±0.0012 was calculated for the UO reaction with authentic urate. The low standard deviation for this KIE measurement showed that the precision of continuous flow MS was sufficient for ^{13}C KIE analysis.

The KIE was again determined by Method II, but this time urate was ^{13}C-depleted at position C4. The KIE at position C5 was found to be 0.9323±0.0097. Because the ^{13}C content of the sample was much higher than the 50% depleted, it was concluded that the glyoxylate analyzed was not pure. Carbon contamination was present. Upon analyzing samples from each step of Method II, Table 2-5, it was determined that 50% of the allantoin was lost when urate and allantoin were separated on the Dowex column. This problem led to the development of Method III.

Method III was developed to completely separate allantoin from the un-reacted urate by using HPLC. The C4-C5 KIE of urate measured using Method III was 1.000±0.004. When this method was used to determine the KIE at position C5 with the ^{13}C-depleted urate, the expected ^{13}C-depletion in the sample was not obtained. This indicated that contamination of the sample with carbon was possible. Therefore, samples collected and solutions used in the reaction were analyzed by ^{1}H NMR. It was found that

the Tris buffer contained an impurity. This impurity was carried through to the glyoxylate sample that was purified for MS.

Method IV eliminated the contamination from the Tris buffer and the need for separation of allantoin by HPLC. Phosphate buffer was found to be compatible for the UO reaction, eliminating the carbon contamination found in the Tris buffer. Since the separation of allantoin was very time consuming, hydantoinase was used to catalyze the reaction of allantoin to allantoate. The C4-C5 KIE measured using Method IV was 0.9967±0.002. When the C5 KIE was measured utilizing the ^{13}C-depleated substrate, there was less contamination, but the ^{13}C-depletion in the sample was still almost half the expected amount.

The intrinsic isotope effect along with the apparent KIE can be used to model the transition state structure of a reaction mechanism (Warshel *et. al.,* 2006). Therefore, determination of the intrinsic isotope effect is important in mechanistic studies. By plotting the effect of the KIE values with respect to substrate concentration and interpolating to zero concentration, the intrinsic isotope effect can be estimated. To determine the intrinsic isotope effect, oxygen's KIE was determined under 5, 10, 20, and 100% oxygen atmospheres. The ^{18}(V/K) was plotted with respect to oxygen concentration. A trend was observed in the data, but when MS analysis was repeated on the samples the oxygen content had risen dramatically. This change in water content changed the observed KIE for the same samples (Table 2-4). TGA was used to analyze the water content of the sample. The result confirmed our suspicion that the sample had absorbed water, even though it was stored in a vacuum desiccator. Most likely NaOH, used to elute glyoxylate during purification, was absorbing water. In order to reduce the

hydrophilicity of the samples, different salts were compared by TGA. It was found that KCl was much less hydrophilic. Therefore, we repeated the ^{18}(V/K) measurement eluting the allantoin with a KCl solution instead of LiCl. This greatly decreased the amount of water in the samples. When ^{18}(V/K) was plotted vs. oxygen concentration, a trend was observed (Figure 2-9). As the amount of substrate is increased the apparent KIE should be reduced. When the data was plotted, the KIE did not approach 1.0 as expected with increased oxygen concentration. Even though a trend was observed for the ^{18}(V/K) data, the sample error resulted in all values to be considered equivalent. There are two likely possibilities for this result: water contamination skewing the ^{18}(V/K) values or the oxygen concentration did not affect the KIE.

In conclusion, the investigations here build a foundation for the development of novel methods to measure KIE using continuous flow MS. We have shown that continuous flow MS can accurately measure the isotopic ratio of a compound with the precision required for KIE's. Advances in the development of a method to measure ^{13}(V/K) KIE of the UO reaction at the C4 and C5 positions of urate have been made. These advances include the development of a method that combined enzymatic and chemical steps to degrade the UO reaction product to glyoxylate. Another advancement is in the use of ^{13}C-depleted substrate to determine the ^{13}(V/K) KIE of a single carbon in a complex molecule. Problems with background contamination prevented us from measuring the actual value for ^{13}(V/K). There are still several possible directions for the measurement of the ^{13}(V/K) for C4 and C5 of urate. The first would be to use Method IV to prepare glyoxylate samples. The reaction mixture could be injected directly into an HPLC/UPLC MS which could isolate and analyze glyoxylate in one step. Another

possibility would be to prepare glyoxylate samples as in Method IV and measure the isotopic ratio of CO_2 as in Method I. By combining these methods, all steps could be completed in one vessel without the risk of introducing contamination from a column or solvent. Finally, advanced electrospray MS is making it possible for the determination of the isotopic ratio at each position of complex molecules (Cassano *et. al*., 2007). This technology may make KIE measurements for complex molecules much simpler. Preliminary experiments for the measurement of whole molecule ^{18}(V/K) KIE of urate for the determination of the intrinsic isotope effect of the UO reaction were also conducted. These experiments show promise if allantoin could be isolated from the reaction without any oxygen contamination from water.

Chapter 3. Proton Inventory

3.1 Introduction

To understand the mechanics of enzymatic reactions is one of the fundamental focuses of enzymology. Understanding how an enzyme can accomplish catalysis can be beneficial in developing inhibitors, determining intermediates, and predicting how similar reactions occur. Urate oxidase (UO) catalyzes the reaction of urate to 5-hydroxyisourate without the aid of a cofactor (Scheme 1-1). This is unusual since most enzymatic oxidation reactions incorporate either a metal or flavin cofactor. This unusual method of oxidation makes UO an excellent choice for the study of its reaction mechanism. A catalytic diad has been previously proposed to play an important role in the UO reaction mechanism (Imhoff *et. al*., 2003). This diad was proposed to abstract a proton from the substrate to form the first intermediate in the UO reaction mechanism, urate dianion. The deprotonation of urate is thought to be facilitated by lysine at position 9 deprotonating a threonine at position 69 and activating it for the abstraction of a proton at the N9 position of urate forming dianionic urate. This proposal predicts that the catalytic diad would be responsible for two protons being in flight for each round of catalysis.

To further investigate the proposed Thr-Lys diad, we have employed the proton inventory method (PI) on the UO reaction mechanism. PI is a kinetic study of solvent isotope effects (SIE) in mixed isotopic waters. Information on the number of protons in flight during a round of catalysis can be determined from proton inventory studies (Schowen *et. al*., 1982). This method was used to determine the number of protons in flight during the catalysis of 6-thiourate with UO. The SIE on the UO reaction with urate

was not large enough to accurately measure a PI for the reaction. The larger the SIE on the reaction the easier it is to distinguish whether there is curvature in the PI. To increase the magnitude of the SIE, the slow substrate 6-thiourate was used. Because 6-thiourate is similar in structure to urate, (Figure 3-1) a similar mechanism for its oxidation would be expected. The reduction in rate of the UO reaction with 6-thiourate compared to urate indicates that the rate limiting step of the reaction is slower. This slower rate limiting step would have a higher energy barrier to overcome. This higher barrier would increase the partitioning of deuterium and hydrogen and thus increase the observed SIE.

Figure 3-1: The structures of urate and 6-thiourate are similar.

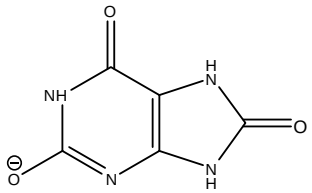

Urate

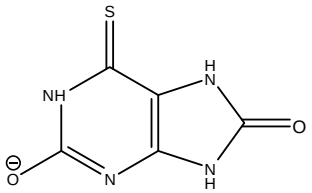

6-thiourate

3.2 Methods

General Procedures and Reagents

Deuterium oxide (99.9 atom D%) was purchased from Aldrich. Buffers MOPSO, MES, HEPES, and TRIS, were purchased from Research Organics Inc. CAPS buffer was purchased from Sigma. Other reagents used have been previously listed in section 2.2.

Mutagenesis and Purification

The construction and purification of UO has been outlined in section 2.2.

Solutions

All 50 mM Tris buffer solutions for the PI studies were prepared by mixing appropriate amounts of 50 mM Tris buffers made in D_2O and H_2O at pL 8.0 or pL 10.0. All pD values were estimated using the relationship pD=pH meter reading + 0.4.

Preparation of 6-thiouric acid

6-thiouric acid was synthesized by heating diamine and urea at 180-200˚C under nitrogen for 30 minutes. The fused mass was dissolved in 5% sodium hydroxide and treated with Norit. The filtrate was acidified with glacial acid and the crude 6-thiourate that precipitated was isolated, washed with water, washed with ethanol, and air dried (Levin, 1960).

Initial Velocity Studies

The initial velocity kinetics V_{max} and K_m of UO with the substrate 6-thiourate were determined in triplicate for solutions containing varying compositions n, where $n=D_2O/H_2O$. The initial velocity was measured by monitoring the disappearance of 6-thiourate spectrophotometrically at 346 nm. All V_{max} and V/K results were estimated

from initial rates of the reactions between UO and the substrate 6-thiourate by nonlinear curve fitting to Michaelis-Menten equation using GraFit 5. The error on V/K was determined by performing a propagation of error calculation. Kinetic studies were performed in the following buffers for the specified pH range: MOPSO pH 5.75-6.25, MES pH 6.25-6.5, HEPES pH 6.5-8.0, TRIS pH 8.0-9.0, and CAPS pH 9.5-11.0.

Fitting of pH Curve

For the pH curve, data was fit using GraFit 5 double bell and single pKa equations. The double bell and singe pKa equations 3-1 and 3-2 respectively, are shown below.

$$y = \frac{Limit.temp1}{10^{(2\,pH - pKa_1 - pKa_2)} + temp1 + 1} \tag{3-1}$$

$$y = \frac{Limit.10^{(pH - pKa)}}{10^{(pH - pKa)} + 1} \tag{3-2}$$

Proton Inventory Calculations

Proton inventories (PI) of the results were plotted as ^{D}V and $^{D}(V/K)$ vs. n to ascertain linearity. Where ^{D}V is the ratio of velocities determined in water and mixed waters n, V_{Water}/V_n, and similarly $^{D}(V/K)=(V/K)_{Water}/(V/K)_n$. The ISOV equation (Equation 3-3) was fit to the PI data for the determination of error values on ^{D}V using GraFit 5.

$$V_{\max} = \frac{V_{\max}[S]}{(K_m + [S])(1 + n^{D}V^{1})} \qquad (3\text{-}3)$$

In equation 3-3 [S] is the concentration of substrate, n is the fraction of D_2O/H_2O, ${}^{D}V_1$ is the SIE on V_{max}. The actual value for ${}^{D}V$ was calculated by adding 1 to the value determined from the ISOV fit.

Analysis of data

Fractionation factors, ø, were determined from fitting of the Gross-Butler equation (Equation 1-7). A fractionation factor is the ratio of heavy to light isotope in the product divided by the ration of heavy to light isotope in the substrate. Equation 3-4 shows the fractionation factor relationship with hydrogen and deuterium.

$$\phi = \frac{\frac{D}{H}\,product}{\frac{D}{H}\,substrate} \qquad (3\text{-}4)$$

Two different types of fractionation factors can play a role in SIE's of enzymatic reactions. A ground state fractionation factor, $ø^{G}$, is due to the hydrogenic exchange occurring before the transition state. The transition state fractionation factor, $ø^{T}$, is a result of proton exchange occurring in the transition state.

Previous theoretical approaches (Theodorou, *et. al*., 2001) were used to determine the significance of PI parameters in the Gross-Butler equation (Equation 1-7). Several equations were fitted to experimental data using GraFit 5. Equation 3-5 describes a situation in which two exchangeable hydrogenic sites have different fractionation factors and all ground state fractionation factors are equal to 1, therefore reducing the denominator to unity. Equation 3-6 describes a case where the exchangeable sites have

identical fractionation factors in the transition state and in the ground state. Equations 3-7, 3-8, and 3-9 are variations in which exchangeable hydrogenic sites have non-identical fractionation factors in the ground state and/or in the transition state.

$$^{D}V = (1 - n + n\phi^{A})(1 - n + n\phi^{B}) \quad (3\text{-}5)$$

$$^{D}V = \frac{(1 - n + n\phi^{A})^{2}}{(1 - n + n\phi^{C})^{2}} \quad (3\text{-}6)$$

$$^{D}V = \frac{(1 - n + n\phi^{A})(1 - n + n\phi^{B})}{(1 - n + n\phi^{C})^{2}} \quad (3\text{-}7)$$

$$^{D}V = \frac{(1 - n + n\phi^{A})^{2}}{(1 - n + n\phi^{C})(1 - n + n\phi^{D})} \quad (3\text{-}8)$$

$$^{D}V = \frac{(1 - n + n\phi^{A})(1 - n + n\phi^{B})}{(1 - n + n\phi^{C})(1 - n + n\phi^{D})} \quad (3\text{-}9)$$

To determine which equation best fitted the data, unweighted nonlinear curve fitting was performed using GraFit 5. The reduced standard deviation of the calculated parameters, along with the Chi^2 test, was used to compare the quality of each fit to the data.

3.3 Results

pH curve with 6-thiourate

Previous pH studies of UO had detected a general acid with a pKa of 6.4 but the pH profiles were not carried out past pH 8.0 (Imhoff *et. al*., 2003). Because there was no data indicating what the effect pH had on the UO reaction above pH 8.0, a more detailed look at the effects of pH on the UO reaction was initiated. Furthermore there were no pH profiles using 6-thiourate. In this study, we conducted PI studies using the slow substrate 6-thiourate at pH 8.0 and 10.0. Therefore, pH kinetics were analyzed for the UO reaction covering a range of pH 6.0-10.5 with the substrates urate and 6-thiourate.

Kinetics were determined in various buffer systems over a pH range of 6.0 to 10.5. The rate of reaction was determined using UV visible spectroscopy at 346nm to monitor the disappearance of 6-thiourate over time. The initial velocity was plotted with respect to concentration of substrate and the Michaelis-Menten equation was used to determine the kinetic values K_m and V_{max}. Next, V_{max} and V/K were plotted vs. pH and GraFit 5 was used to fit a both a single ionization and double bell curve for the determination of pKa values (Equations 3-1 and 3-2). Figures 3-2 and 3-3 show the pH profile for UO with 6-thiourate with the single and double ionization curves fit respectively. By comparing the two fits it can be seen that the double bell curve fits the data best. The pH profile with urate was similar, data not shown. The pKa values determined from the V_{max} profile for UO with 6-thiourate were 6.5±0.1 and 10.3±0.1. For the profile of V/K vs. pH the determined pKa was 6.7±0.3 and 9.6±0.2. Values for pKa are tabulated in Table 3-1.

Table 3-1: Urate Oxidase pKa values for with urate and 6-thiourate

Substrate	Parameter	pKa1	pKa2
Urate	V_{max}	6.9±0.2	10.2±0.2
6-thiourate	V_{max}	6.5±0.1	10.3±0.1
6-thiourate	V/K	6.7±0.3	9.6±0.2

Figure 3-2: The pH profiles of V_{max} and V/K for UO with 6-thiourate fit to a single ionization curve.

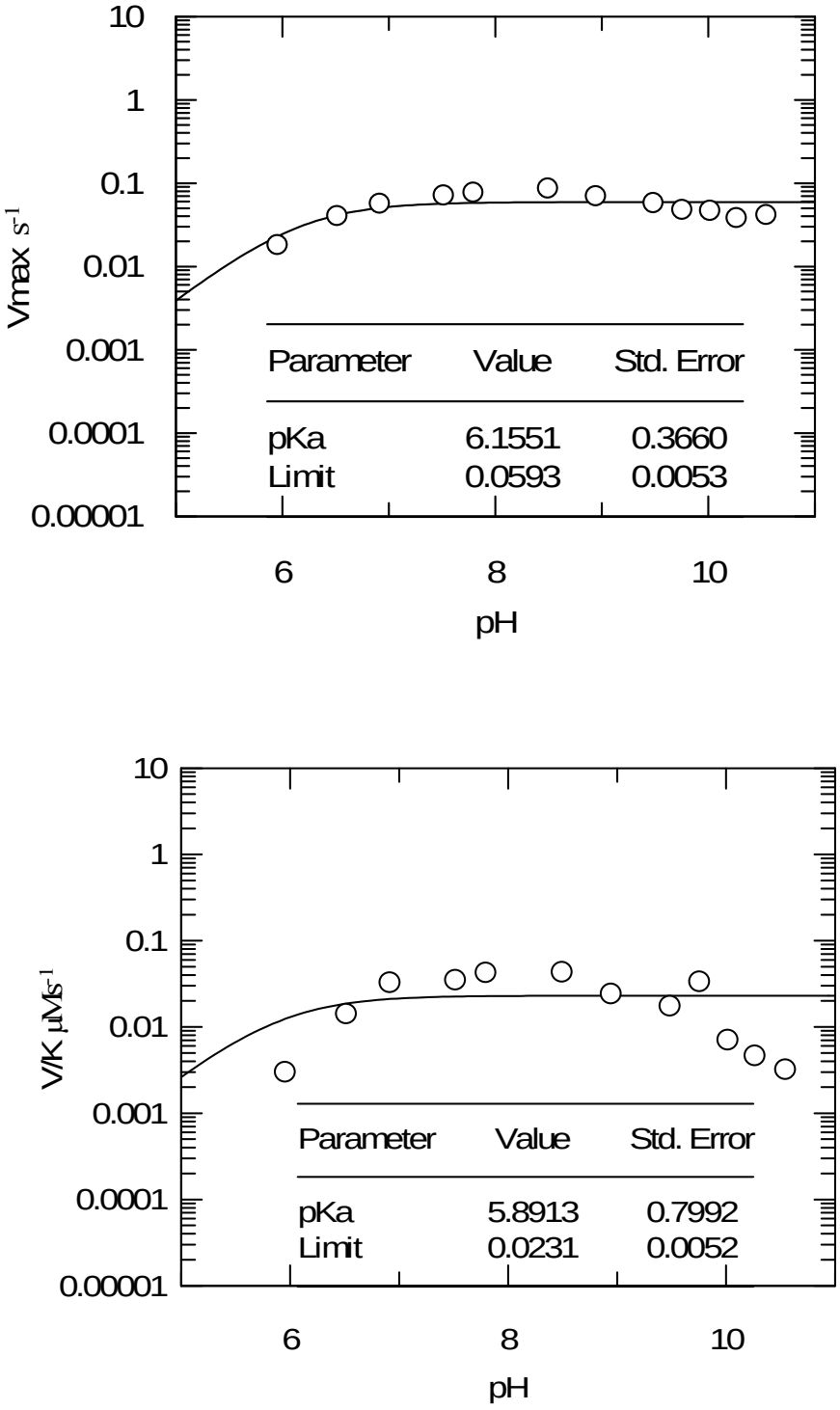

Figure 3-3: The pH profiles of V_{max} and V/K for UO with 6-thiourate fit to a double bell curve.

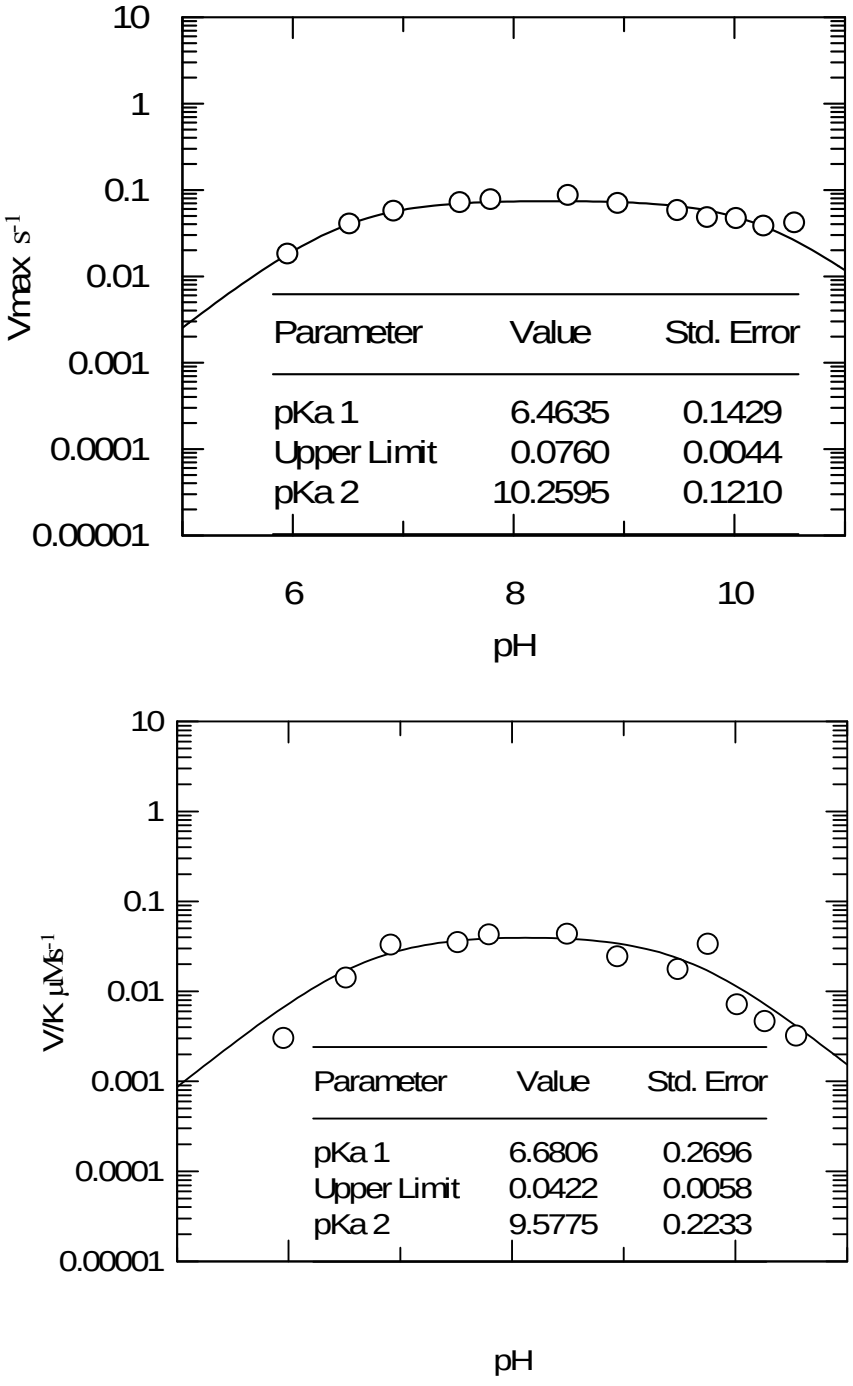

Proton Inventory

The solvent isotope effect on the UO reaction with 6-thiourate in D_2O is ~2, making this reaction a good candidate for PI methods. The magnitude of ^{D}V and $^{D}(V/K)$ were determined at pL 8.0 and 10.0 with 6-thiourate as the substrate in a series of mixed waters consisting of D_2O and H_2O. These values were plotted with respect to n (Figure 3-4, 3-5 and 3-6). The PI for ^{D}V, as seen in Figure 3-4, has a normal isotope effect and is "bowl-shaped". This "bowl-shape" indicates that more than one proton may be in flight during each round of catalysis. The PI for $^{D}(V/K)$ (Figure 3-5) is linear with little or no isotope effect. Interestingly, at pL 10.0 the PI of ^{D}V becomes linear with little or no apparent isotope effect. The PI of $^{D}(V/K)$ at pL 10.0 (Figure 3-6) had an inverse isotope effect and is linear. Protons in flight in portion of the mechanism up to the first irreversible step are detected in $^{D}(V/K)$ PI. Protons in flight after the first irreversible step are measured in the ^{D}V PI. There are two acid and a base exchanges predicated after the first irreversible step in the proposed mechanism for UO (Scheme 3-1)

The Gross-Butler equation is commonly used to analyze PI data for determination of number and type of protons that give origin to curvature in PI data (Theodorou et. al., 2001; Gandour, 1980). To further investigate the "bowl-shaped" PI of ^{D}V at pL 8.0, the Gross-Butler equation was applied. Equation 3-10 is a simplification of the Gross-Butler equation (Equation 1-7) in which the number of protons, y, determine the curvature of the PI. By rearranging Equation 3-10, the straight line equation could be written (Equation 3-11). If the data fits this equation, a straight line would result when $^{1/y}(^{D}V)$ is plotted vs. n. In Figure 3-7, data for ^{D}V was fit to Equation 3-11 with y values of 2, 3, and 4. It was apparent that when y=2 the plot was not linear. When y values of 3 and 4 are used in the

equation, their plots became more linear, but it becomes difficult to determine whether they are truly linear. Therefore, a more robust treatment of the data was needed.

$$^{D}V = (1 - n + n\phi^{A})^{y} \qquad (3\text{-}10)$$

$$^{1/y}(^{D}V) = n\phi^{A} + 1 - n \qquad (3\text{-}11)$$

Non-linear best fitting was used to determine which form of the Gross-Butler equation most closely represented the "bowl-shaped" PI for ^{D}V at pH 8.0. GraFit 5 was used to fit Equations 3-5 through 3-9 to ^{D}V vs. n. Fitting to Equation 3-5 did not return good fits to the data. In Figure 3-8, a value of y=2 is shown, y=3 and 4 were also used (data not shown). Because these simple models did not match the data, other factors than the transition state fractionation factor, ϕ^{T}, must be contributing to the "bowl-shaped" PI, or $\phi^{G} \neq 1$. Therefore, curve fitting of Equations 3-6 to 3-9, in which ground state fractionation factors were not equal to one are taken into consideration (Figures 3-9 to 3-12). When fit to Equation 3-6, assuming that the two fractionation factors due to the transition state were equal as well as the two fractionation factors in the ground state being equal, the curve fit the data well (Figure 3-9). The fractionation factors for this equation were: ϕ^{A}=0.5543 and ϕ^{C}=0.3914, with a reduced Chi^2 value of 0.0027.

Figure 3-4: The ^{D}V PI for UO with 6-thiouarte at pL 8.0 is "bowl-shaped". This bowl shape is indicative of more than one proton being in flight during the transition state of the reaction mechanism. The straight line is used to show the curvature of the data.

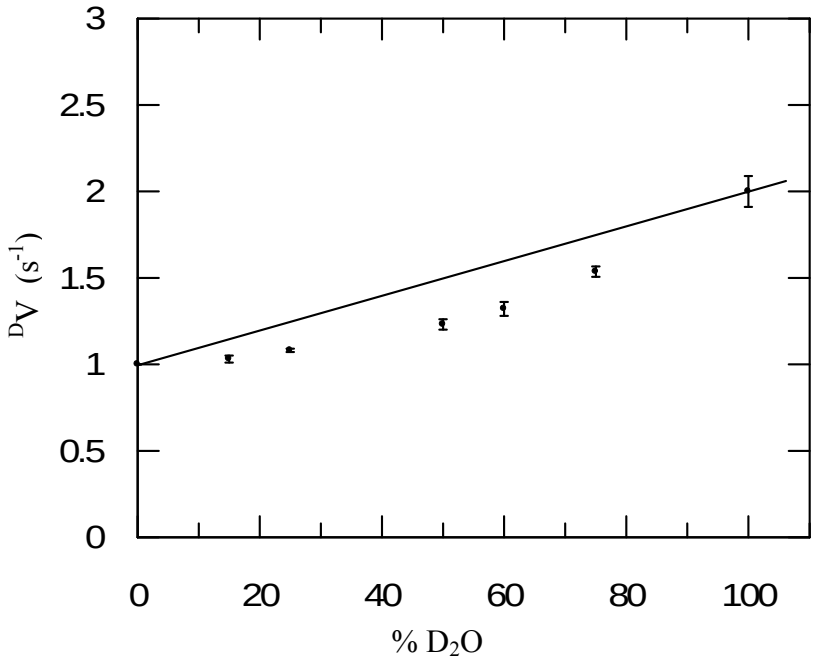

Figure 3-5: The ^{D}(V/K) PI is linear at pL 8.0.

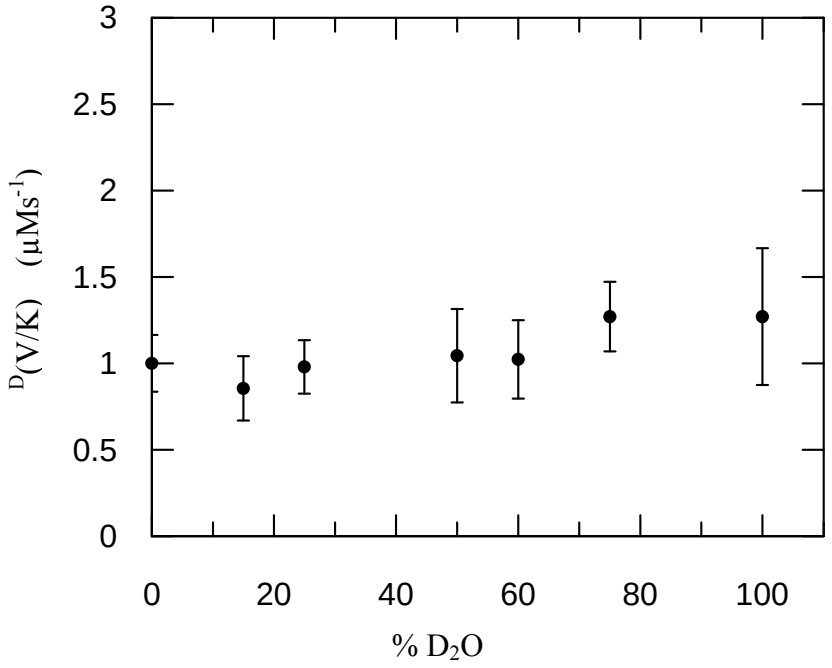

Figure 3-6: ^{D}V and $^{D}(V/K)$ PI for UO at pL 10.0.

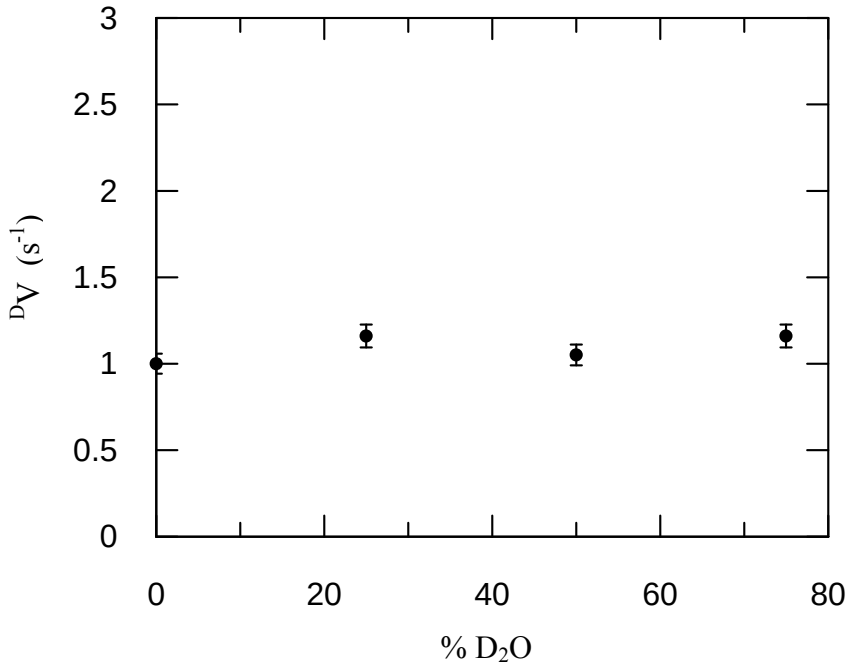

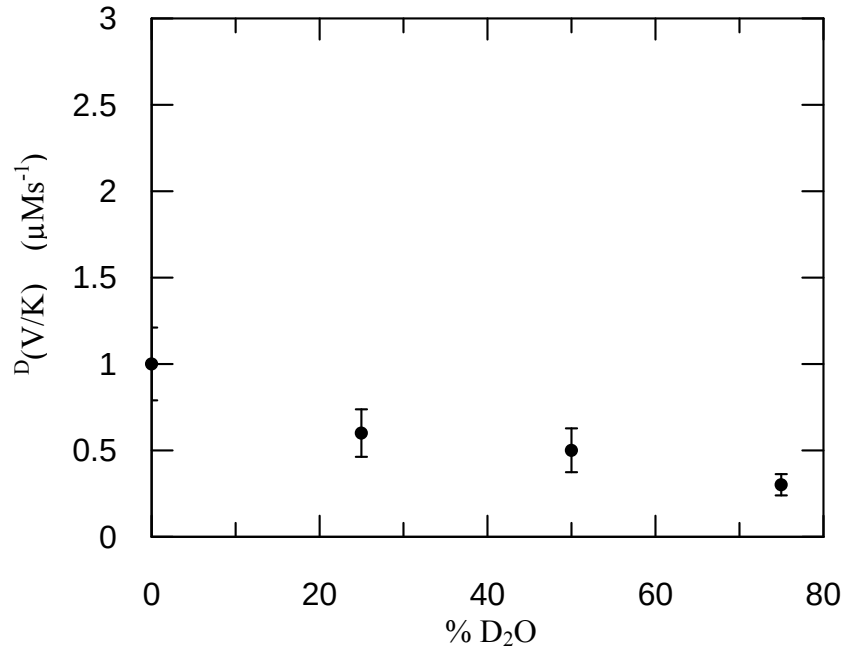

Figure 3-7: Comparison of squared, cubed and 1/4 root functions fit to Equation 3-10. A plot of the square root of the ^{D}V was not linear as would be expected for a PI due to 2 protons in flight. Factors other than the number of protons in flight may account for bowl shape PI. Plots of $^{D}V^{(1/3)}$ and $^{D}V^{(1/4)}$ are not linear either.

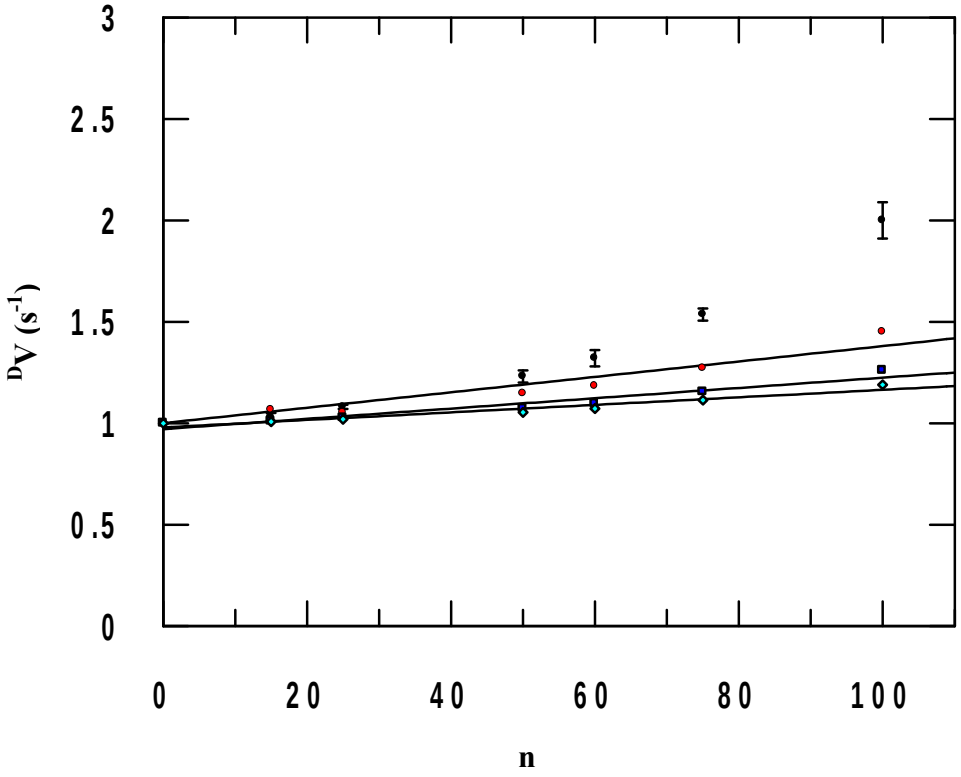

Figure 3-8: Fit of the PI data to Equation 3-5 which assumes ϕ_G=1 and that 2 protons are in flight.

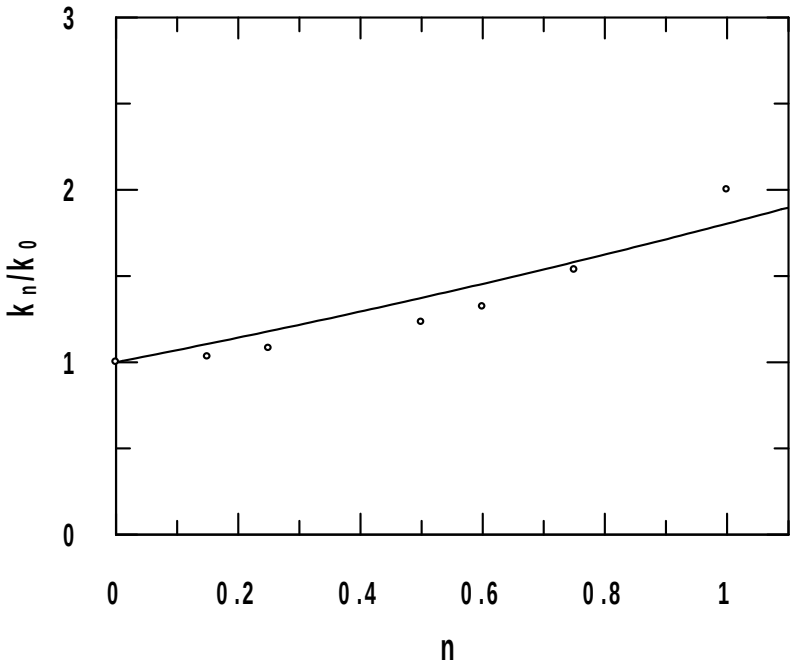

Chi²: 0.0943

Parameter	Value	Std. Error
A	1.3776	0.1691
B	1.3090	0.1600

Figure 3-9: PI data fit to Equation 3-6.

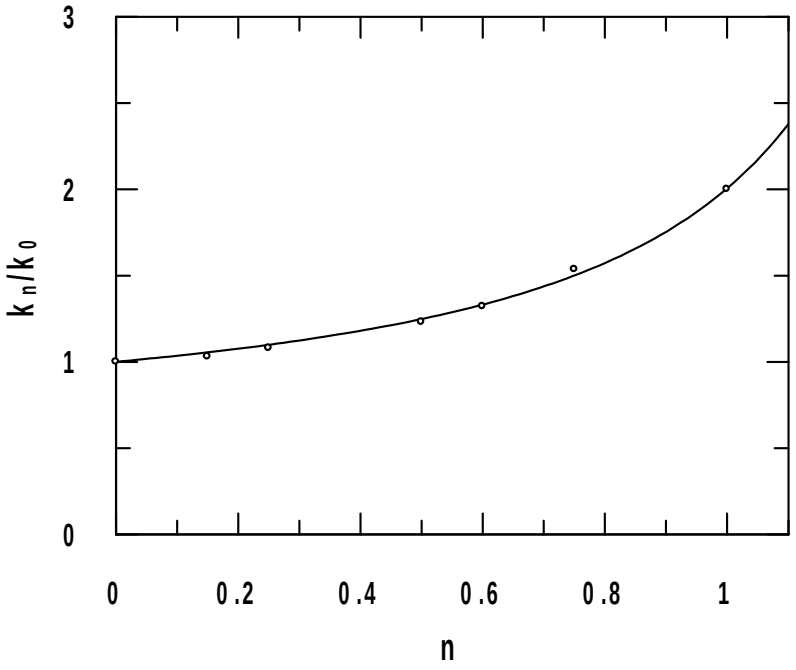

Chi²: 0.0027

Parameter	Value	Std. Error
A	0.5543	0.0355
C	0.3914	0.0261

Figure 3-10: PI data fit to Equation 3-7.

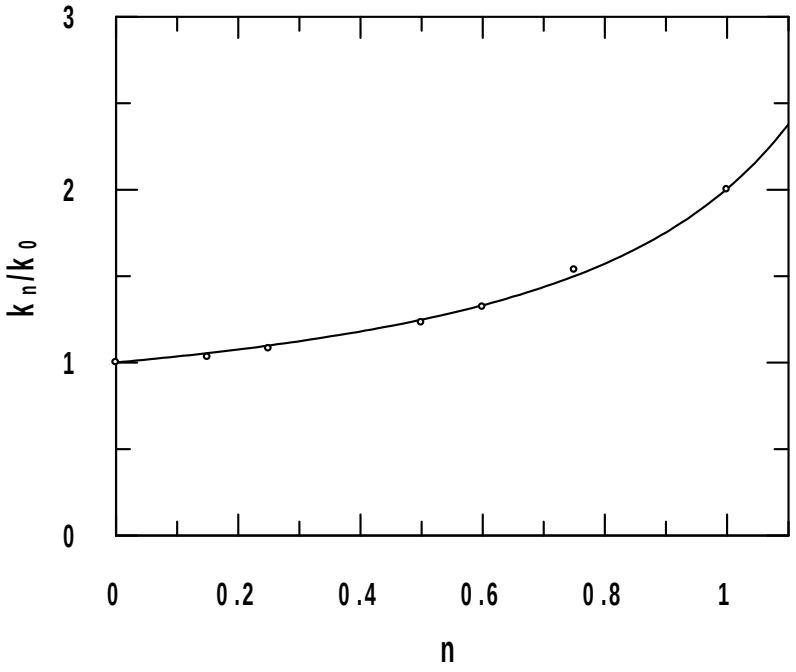

Chi²: 0.0027

Parameter	Value	Std. Error
A	0.5509	136.0740
B	0.5577	136.0740
C	0.3914	0.0292

There was a good fit to Equation 3-7 (Figure 3-10), in which there were two separate fractionation factors in the transition state and one in the ground state. The values determined from this equation were: ϕ^A=0.5543, ϕ^B=0.5577, and ϕ^C=0.3914, with a reduced Chi^2 value of 0.0027. These values were very similar to the values obtained for Equation 3-6. Since ϕ^A and ϕ^B were essentially the same when fit to Equation 3-2, it can be reasonably assumed that equations 2-3 and 3-3 yield the same result. When the data was fit to Equation 3-8 there is also a good fit (Figure 3-11) with values for ϕ^A, ϕ^C, and ϕ^D of 0.5543, 0.4001, and 0.3827 respectively and a reduced Chi^2 value of 0.0027. Lastly, a fit of Equation 3-9 is shown in Figure 3-12. The fractionation factors calculated from this plot were ϕ^A=1.5174, ϕ^B= 1.5018, ϕ^C = 0.4557, and ϕ^D = 2.4981 with a reduced Chi^2 value of 0.0005. These fractionation values did not fall in the range of values expected for acid-base catalysis (Albery, 1975). Therefore, Equation 3-9 did not adequately represent the data. It is standard practice to assume that if no significant difference exists between two models that the simplest model that reasonably describes a system is preferred (Mannervik, 1982). Since equations 3-6 and 3-8 both describe the PI for ^{D}V with similar reduced Chi^2 values, the more basic equation, Equation 3-6, best describes the data. Parameter estimates and reduced Chi^2 values are tabulated in Table 3-2 below.

Table 3-2: Parameter Estimates for Proton Inventories of ^{D}V

Equation	ϕ^A	ϕ^B	ϕ^C	ϕ^D	Chi^2
3-5	1.3776	1.3090	NA	NA	0.0943
3-6	0.5543	NA	0.3914	NA	0.0027
3-7	0.5509	0.5577	0.3914	NA	0.0027
3-8	0.5543	NA	0.4001	0.3827	0.0027
3-9	1.5174	1.5018	0.4557	2.4981	0.0005

Figure 3-11: PI data fit to Equaiton 3-8.

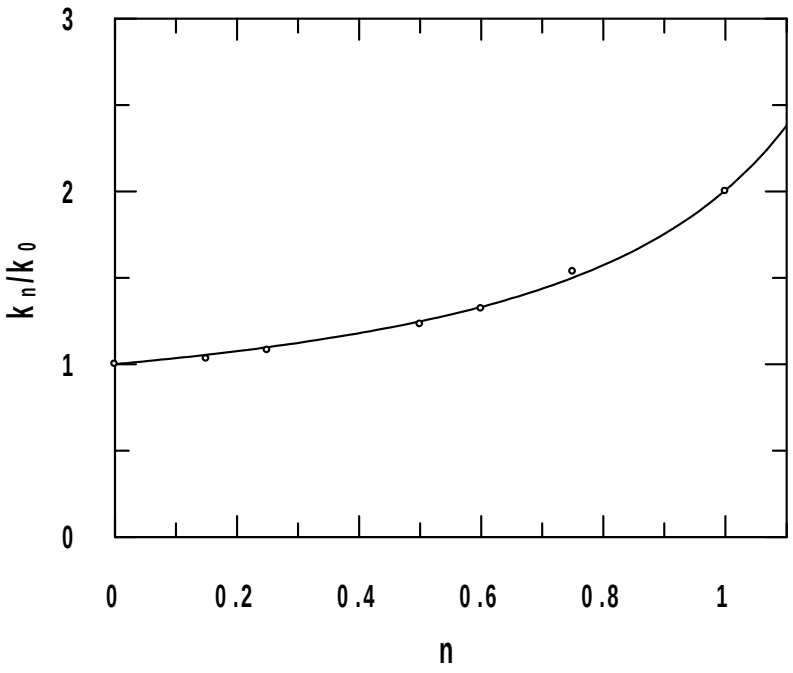

Chi^2: 0.0027

Parameter	Value	Std. Error
A	0.5543	0.0397
C	0.4001	100.1147
D	0.3827	100.1148

Figure 3-12: Fit of PI data to Equation 3-9.

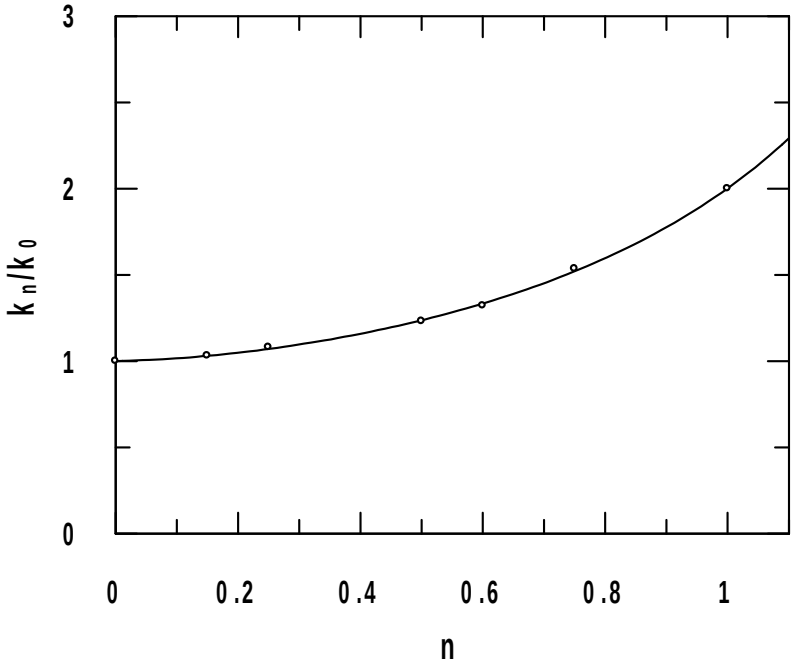

Chi^2: 0.0005

Parameter	Value	Std. Error
A	1.5174	16.9601
B	1.5018	16.9617
C	0.4557	0.0324
D	2.4981	0.4295

3.4 Discussion

A complete pH curve was determined for UO with 6-thiourate. Previously, pH studies had only been carried out to pH 8.0. To determine if the pKa of 6-thiourate differed from that of urate with UO, a pH profile covering the complete active pH range of UO was conducted. Figure 3-3 shows profiles for V_{max} and V/K with respect to pH. Two pKa values were determined from the V_{max} profile for UO with 6-thiourate 6.5±0.1 and 10.3±0.1. For the profile of V/K vs. pH the determined pKa was 6.7±0.3 and 9.6±0.2. Values for pKa are tabulated in Table 3-1. The pKa values of 6.5 and 6.7 agree with previously published data (Imhoff *et. al*., 2003). In addition, there is evidence of a catalytic acid with a pKa of ~10 that was not evident from the earlier pH profile.

Two protons would be expected to be in flight due to the proposed Thr-Lys catalytic-diad during a round of catalysis. To investigate the number of protons in flight the proton inventory method was used. PI is an accepted method that uses SIE to dissect information about the transition state structure and number of protons in flight during catalysis of a reaction mechanism (Schowen, 1982). The UO reaction with 6-thiourate has a SIE on V_{max} of ~2. A SIE of 2 is consistent with acid-base catalysis according to Schowen's "salvation catalysis" model in non-enzymatic systems (Quinn, 1980). PI of UO with the slow substrate 6-thiourate was used increase the magnitude of the SIE over that of urate. Because the SIE is larger with 6-thiourate, any curvature in the PI was much easier to ascertain.

The PI for ^{D}(V/K) at pH 8.0 was linear with an SIE of ~1. ^{D}(V/K) detects protons in flight from all steps from binding of the substrate to enzyme up until the first irreversible step of the reaction (Kiick, 1991). Because there was no SIE on ^{D}(V/K) and

there was a SIE for ^{D}V, the isotopic sensitive step was determined to be after the first irreversible step. If the Thr-Lys catalytic diad is involved in the first irreversible step as expected, the formation of the hydroperoxide intermediate, it would not responsible for the "bowl shaped" PI o f ^{D}V. Scheme 3-1 shows proposed general acid (GA) and general base (GB) steps of the UO catalytic pathway along with the portions of the reaction that are detected by ^{D}V and $^{D}(V/K)$.

Scheme 3-1

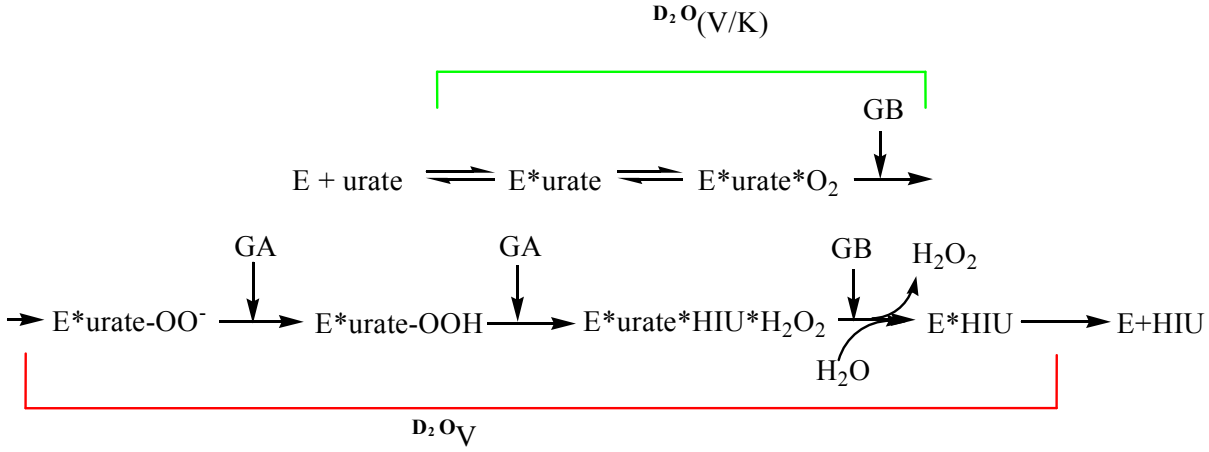

The PI for ^{D}V at pH 8.0 was "bowl-shaped", indicating that more than one proton was involved in a single round of catalysis. A simplified form of the Gross-Butler equation in which the ground state fractionation factor is assumed to be equal to one was fit to the PI (Equation 3-5). This equation gave a ^{D}V with a curvature that was less than adequate to fit the data (Figure 3-8). Equation 3-11, which also assumes a ground state fractionation of unity, was also used to fit PI data for ^{D}V. Results with the number of protons in flight, y, set equal to 2, 3, and 4 gave similar results to that of equation 3-11 (Figure 3-7). Since these simplified versions of the Gross-Butler equation did not provide an explanation of the data, solvent reorganization may not be the only event responsible

for ground state proton exchange. Therefore, the presence of discrete non-unit fractionation factors in the ground state was needed to fit the Gross-Butler equation to the data. Several forms of the Gross-Butler equation which take into account the ground state fractionation factors were fit to the PI data for comparison. The results for these fittings are tabulated in Table 3-2. After comparing the fractionation factor values, standard deviation, and factoring in the reduced Chi^2 of the fit, Equation 3-6 was concluded to be the best approximation of the experimental data for ^{D}V. The fractionation factor values for this equation were: ϕ^{A}=0.5543 and ϕ^{C}=0.3914, with a reduced Chi^2 of 0.0027. According to this model, the isotope effect was due to two exchangeable protons in the transition state and two in the ground state. Albery (Quinn, 1980) has suggested ranges of the magnitude of transition state fractionation factor values for different cases. These limits may be used to understand the meaning of fractionation factors determined from experimental data. Values of $\phi_T < 0.3$ are an indication that a proton transfer between two atoms is occurring. If $0.4 < \phi_T < 0.7$, then vibrational coupling between heavy atom reorganization (HAR) and proton transfer (PT) is occurring. A $\phi_T > 0.7$ implies that the proton is not translating in the transition state. Since the transition state fractionation factor for ^{D}V was ϕ_T=0.5543, it can be proposed that this is due to vibrational coupling between HAR and PT. These observations are consistent with a multi-proton catalytic chain such as occurs in amidohydrolases and serine proteases (Quinn, 1980). Proton transfer during the release of H_2O_2 from the urate hydroperoxide intermediate may be responsible for the "bowl shaped" PI of ^{D}V at pH 8.0. Ground state fractionation factors occur from proton exchange in the ground state. The ground state of the reaction is free substrate and free enzyme (Theodorou, 2001). Often times the ground state fractionation

factor is only due to bulk proton exchange with solvent which averages out to give $\emptyset_G$=1, reducing the denominator of the Gross-Butler equation to unity (Equation 3-5). The ground state fractionation factor of 0.3914 may be due to the protonation and/or deprotonation steps that occur to the product or the enzyme before the rate limiting step (Scheme 3-1). Alternatively, low barrier hydrogen bonding (LBHB) may exist within the active site of the enzyme. LBHB may form during the reaction which could account for the ground state fractionation (Schoitt 1998). A LBHB occurs when a hydrogen bond length is decreased, becoming stronger. When this occurs, the hydrogen bond becomes more covalent in nature, essentially sharing two covalent bonds [H-O-H-O-H] (Cleland, 1998). Formation of a LBHB increases the O-H bond length from ~1.0 to ~1.2Å. The bond order decreases and discrimination against deuterium increases (Cleland, 1998). Ground state fractionation factors due to LBHB have been measured as low as 0.3 (Cleland, 1998). LBHB formation by the proposed Lys-Thr catalytic diad could be responsible for a ground state fractionation factor of 0.3914. A proposed structure for this LBHB between Lys-Thr is shown below in Scheme 3-2.

Scheme 3-2:

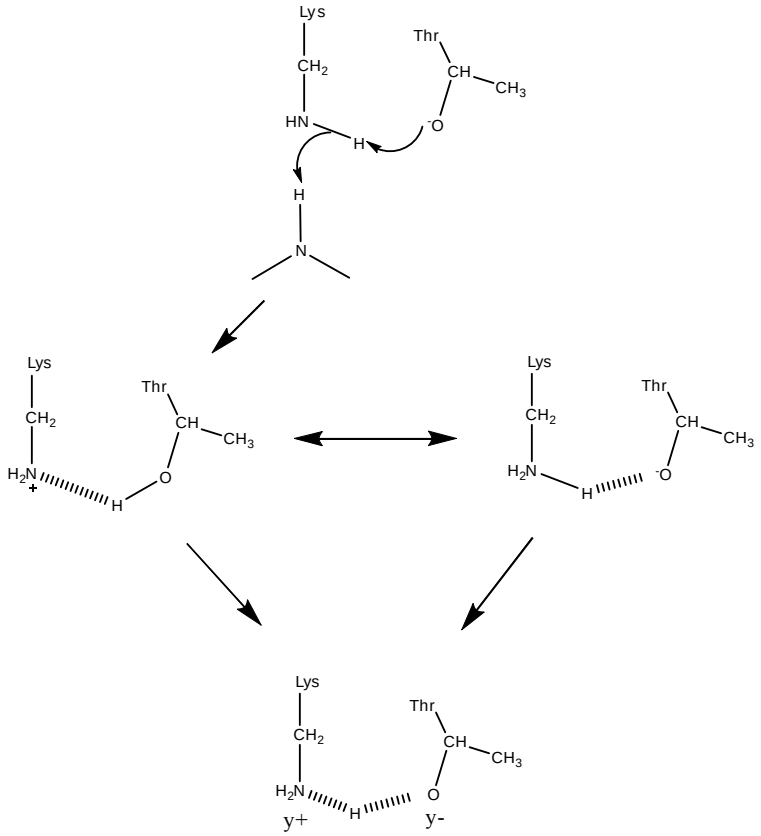

Another possible explanation for the complex fit of the data to the Gross-Butler equation may be that commitment factors have an effect on the magnitude of the SIE. Commitment factors give information on the partitioning of reactant toward substrate or product, C_r and C_f respectively (Karsten & Cook, 2006). Larger forward commitment factors have been shown to decrease the curvature of the PI from a simple model instead of ground state fractionation factors (Kiick, 1991). The relationship of between ^{D}V and commitment factors is demonstrated in Equation 3-12.

$$^{D}V = \frac{^{D}k_n + C_f + C_r(^{D}K_{eq})_n}{1 + R_f / E_f + C_f} \qquad (3\text{-}12)$$

Where $^{D}k_n$ is the partial intrinsic SIE, $(^{D}K_{eq})_n$ is the partial equilibrium SIE, R_f is the catalytic ratio, and E_f is the equilibrium preceding catalysis.

At pL 10.0, ^{D}V becomes linear with respect to n, indicating that only one proton was in flight during catalysis. If the substrate were deprotonated at the N7 position, only one proton would be in flight during the release of H_2O_2. The deprotonation of N7 at pH 10 could account for fewer protons being transferred and the linearity of the ^{D}V PI. Another possibility is that threonine is deprotonated at pL 10.0. In this case, lysine would not be extracting a proton from threonine. Therefore the number of protons in flight would be reduced. At pL 10.0, $^{D}(V/K)$ had an inverse and linear PI. This inversely linear PI may be accounted for by differences in ionization of hydrogen and deuterium. The pKa's of ionizable groups shift upward in D_2O compared to H_2O (Resiga, 2003), These shifts in pKa are generally about 0.45 but can be much larger (Krezel, 2003). This effect could account for the inverse SIE at high pL. Since the second pKa of UO is ~10, at pL 10 the ionizable group would be mostly deprotonated. Since the pKa would be greater than 10 in D_2O, the ionizable group would be mostly protonated at pL 10.0. The state of protonation may effect the binding of substrate causing the reaction in H_2O to be slower that in D_2O. Therefore the SIE would become increasingly inverse as the proportion of D_2O was increased.

The PI data presented here gives further support for the previously proposed reaction mechanism for UO. Curvature in the ^{D}V PI indicates that at least one proton is in flight after the rate limiting step of the reaction. Scheme 3-1 illustrates that there are

several proton transfers that occur after the first irreversible step that could be responsible for the "bowl shaped" ^{D}V PI.

Although in the previously proposed mechanism the Thr-Lys catalytic diad was thought to extract a proton from the substrate activating it for attack on oxygen. A higher resolution crystal structure of UO with the substrate bound flipped with respect to an earlier structure has been published (Retailleau, 2005). This reorientation of the substrate led to a new proposal of how the catalytic diad may facilitate catalysis (Scheme 3-3). In this scheme a base extracts a proton from the N9 position of the substrate. The N9 electrons reorientation facilitates an attack on O_2 to for a urate peroxide radical. Rapidly the peroxide radical would attack the lysine proton and another proton would be transferred from threonine to lysine. This would place the involvement of the catalytic diad after the first irreversible step. Therefore the curvature in the ^{D}V and not in the $^{D}(V/K)$ PI is supportive of the Thr-Lys catalytic diad according to this new proposal.

Scheme 3-3:

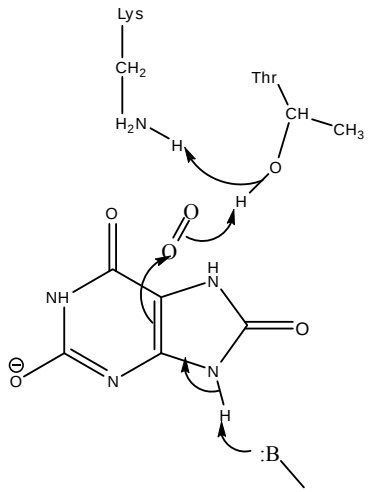

References

Albery, W., J., *In Proton Transfer Reactions*; Gold, V., Caldin, E.: Chapman and Hall: London, (1975).

Breinlinger, E. C., Rotello,V. M., (1997) *J. Am. Chem. Soc.* 119, 1165-1166

Cassano, G. A., Wang, B., Anderson, D. R., Previs, S., Harris, M. E., Anderson, V. E., (2007) *Anal Biochem*. 367(1), 28-39.

Chaney, A. L., (1962) *Clin. Chem*. 8, 130-132.

Cleland W. W., In *Isotope Effects in Chemistry and Biology*; Kohen, A., Limbach, H.; Ed.; CRC Press: Boca Raton, (2006) Chapter 37.

Cleland, W. W., (1987) *Bioorganic Chemistry* 15, 283-302.

Cleland, W. W., Andrews, J. T., Gutteridge, S., Hartman, F. C., Lorimer, G. H., (1998) *Chem. Rev*. 98, 549-561.

Cleland, W. W., Frey, P. A., Gerlt, J. A., (1998) *J. Biol. Chem*. 273, 25529-25532.

Colloc'h, N., Hajji, M., Bachet, B., L'Hermite, G., Schilitz, M., Prang, T., Castro, B., Mornon, J. (1997) *Nature Structural Biology* 4, 3619-3624.

Colloc'h, N., Mornon, J. P., Camadro, J. M., (2002) *FEBS Letters* 526, 5-10.

Davidson, J. N., (1942) Biochem. J. 36, 252-258.

Doll, C., Bell, A. F., Power, N., Tonge, P. J., Tipton, P. A., (2005) *Biochemistry* 44, 11440-11446.

Gandour, R. D., Coyne, M., Stella, V. J., Schowen, R. L., (1980) J. Org. Chem. 45, 1733-1737.

Hoefs, Stable Isotope Geochemistry p22, 1997 Springer-Venlag Berke Heidelberg, Germany

Imhoff, R. D., Power, N. P., Borrok, J. M., Tipton, P. A., (2003) *Biochemistry* 42, 4094-4100

J. Hayes, *Spectra* **8,** 3 (1982)

Holmberg, C. G., (1939) *Biochem*. 120, 1901-1906.

Kahn, K., Serfozo, P., Tipton, P. A., (1997) *J. Am. Chem. Soc.*119, 5435-5442.

Kahn, K., Tipton, P. A., (1997) *Biochemistry* 36, 4735-4738.

Kahn, K., Tipton, P. A., (1998) *Biochemistry* 37, 11651-11659.

Kakino, J., Sato, R., Naito, Y., (1998) *J. Vet. Med. Sci*. 60, 203-206.

Kaltwasser, H., (1971) *J. Bacteriol*, 780-786.

Karsten, W. E., Cook, P. F., In *Isotope Effects in Chemistry and Biology*; Kohen, A., Limbach, H.; Ed.; CRC Press: Boca Raton, 2006; Chapter 30.

Keillin, D., Hartree, E. F., (1936) Proc. Roy. Soc. Lon. Biologic. Sci. 119, 114-140.

Kiick, D., M., (1991) *J. Am. Chem. Soc.* 113, 8499-8504.

Krezel, A., Bal, W., (2003) *J. Inorganic Biochemistry* 98, 161-166.

Kubala, M., Teisinger, J., Ettrich, R., Hofbauerova, K., Kopecky, V., Baumruk, V., Krumscheid, R., Plasek, J., Schoner, W., Amler, E., (2003) *Biochemistry* 42, 6446-6452.

Kurtz, K. A., Rishavy, M. A., Cleland, W. W., Fitzpatrick, P. F., (2000) *J. Am. Chem. Soc*. 122(51), 12896-12897.

LaReau, R. D., Wan, W., Anderson, V. E., (1989) *Biochemistry* 28, 3619-3624.

Levin, G., Kalmus, A., Bergman, F., (1960) *J. Org. Chem*. 25, 1725-1754.

Mahler, H. R., Hubscher, G., Baum, H., (1955) *J. Biol. Chem*. 216, 625-641.

Mannervik, B., (1982) *Methods in Enzymology*, vol. 87, 370-390.

Massey, V. (1994) *J. Biol. Chem*. 269, 22459-22462.

Matthews, D. E., Hayes, J. M., (1979) *Analytical Chem*. 50, 1465-1473.

Oda, M., Satta, Y., Takenaka, O., Takahata, N., (2002) *Mol. Biol. Evol*. 19, 640-653.

O'Leary, M. H., (1980) *Methods in Enzymology* 64, 83-104.

Ortlund, E., Lacount, M. W., Lewinski, K., Lebioda, L., (2000) *Biochemistry* 39(6), 1199-1204.

Patte, C., Sakioglu, C., Anoborlo, A., Baruchel, A., Plouvier, E., Paquement, H., Babin-Boiletot, A., (2002) *Annals of Oncology* 13, 789-795.

Quinn, D. M., Venkatasubban, K. S., Kise, M., Schowen, R. L., (1980) J. Am. Chem. Soc. 102, 5365-5369.

Resiga, D. S., Nowak, T., (2003) J. Biol. Chem. 278, 12660-12671.

Retailleau, P., Colloc'h, N., Vivares, F. B., Castro, B., Hajji, M. E., Prange, T., (2005) Biological Crystallography D61, 218-229.

Sarma, A. D., Tipton P. A., (2000) *J. Am. Chem. Soc*. 122, 11252-11253.

Schiott, B., Iverson, B. B., Madsen, G. K. H., Larsen, F. K., Bruice, T. C., (1998) *Proc. Natl. Acad. Sci*. 95, 12799-12802.

Schowen, K. B., Schowen, R. L., (1982) *Methods Enzymol.* 87, 551-606.

Schuler, W., Reindel, W., (1933) *Z. Physiol. Chem*. 215, 258-266.

Shen, B., Hutchinson, R. C., (1993) *Biochemistry* 32, 6656-6663.

Smith, P. M. C., Atkins, C. A., (2002) *Plant Physiology* 128, 793-802.

Szaweski, R. J., Wharton, C. W., (1981) Biochem. J. 199, 681-692.

Theodorou, L. G., Lymperopoulos, K., Bieth, J. G., Papamicheal, E. M. (2001) *Biochemistry* 40, 3996-4004.

Vogels, G. D., Van Der Drift, C. (1969) *Recueil* 88, 931-

Warshel, A., Olsson, M. H. M., Villa-Freixa, J., In *Isotope Effects in Chemistry and Biology*; Kohen, A., Limbach, H.; Ed.; CRC Press: Boca Raton, 2006; Chapter 23.

Weiss, P. M., (1991) *Enzyme Mechanisms from Isotope Effects, CRC Press*, 291-310.

Zhang, L. H., Duan, J., Xu, Y., Dolier, W. R. (1998) *Tetrahedron Letters* 39, 9621-9622.